

Unusual Structure, Fluxionality, and Reaction Mechanism of Carbonyl Hydrosilylation by Silyl Hydride Complex $[(\text{ArN}=\text{)Mo}(\text{H})(\text{SiH}_2\text{Ph})(\text{PMe}_3)_3]$ Andrey Y. Khalimon,^[a] Stanislav K. Ignatov,^[b] Andrey I. Okhupkin,^[b] Razvan Simionescu,^[a] Lyudmila G. Kuzmina,^[c] Judith A. K. Howard,^[d] and Georgii I. Nikonov*^[a]

Dedicated to Professor Philip Mountford on the occasion of his 50th birthday, and in recognition of his significant contribution to imido chemistry and catalysis

Abstract: The reactions of bis(borohydride) complexes $[(\text{RN}=\text{)Mo}(\text{BH}_4)_2(\text{PMe}_3)_2]$ (**4**: $\text{R} = 2,6\text{-Me}_2\text{C}_6\text{H}_3$; **5**: $\text{R} = 2,6\text{-iPr}_2\text{C}_6\text{H}_3$) with hydrosilanes afford new silyl hydride derivatives $[(\text{RN}=\text{)Mo}(\text{H})(\text{SiR}'_3)(\text{PMe}_3)_3]$ (**3**: $\text{R} = \text{Ar}$, $\text{R}'_3 = \text{H}_2\text{Ph}$; **8**: $\text{R} = \text{Ar}'$, $\text{R}'_3 = \text{H}_2\text{Ph}$; **9**: $\text{R} = \text{Ar}$, $\text{R}'_3 = (\text{OEt})_3$; **10**: $\text{R} = \text{Ar}$, $\text{R}'_3 = \text{HMePh}$). These compounds can also be conveniently prepared by reacting $[(\text{RN}=\text{)Mo}(\text{H})(\text{Cl})(\text{PMe}_3)_3]$ with one equivalent of LiBH_4 in the presence of a silane. Complex **3** undergoes intramolecular and intermolecular phosphine exchange, as well as exchange between the silyl ligand and the free silane. Kinetic and DFT studies show that the intermolecular phosphine exchange occurs through the predissociation of a PMe_3 group, which, surpris-

ingly, is facilitated by the silane. The intramolecular exchange proceeds through a new non-Bailar-twist pathway. The silyl/silane exchange proceeds through an unusual Mo^{VI} intermediate, $[(\text{ArN}=\text{)Mo}(\text{H})_2(\text{SiH}_2\text{Ph})_2(\text{PMe}_3)_2]$ (**19**). Complex **3** was found to be the catalyst of a variety of hydrosilylation reactions of carbonyl compounds (aldehydes and ketones) and nitriles, as well as of silane alcoholysis. Stoichiometric mechanistic studies of the hydrosilylation of acetone, supported by DFT calculations, suggest the operation of an unexpected mechanism, in that the silyl

ligand of compound **3** plays an unusual role as a spectator ligand. The addition of acetone to compound **3** leads to the formation of $[\textit{trans}\text{-}(\text{ArN})\text{Mo}(\text{O}i\text{Pr})(\text{SiH}_2\text{Ph})(\text{PMe}_3)_2]$ (**18**). This latter species does not undergo the elimination of a Si–O group (which corresponds to the conventional Ojima's mechanism of hydrosilylation). Rather, complex **18** undergoes unusual reversible $\beta\text{-CH}$ activation of the isopropoxy ligand. In the hydrosilylation of benzaldehyde, the reaction proceeds through the formation of a new intermediate bis(benzaldehyde) adduct, $[(\text{ArN}=\text{)Mo}(\eta^2\text{-PhC}(\text{O})\text{H})_2(\text{PMe}_3)]$, which reacts further with hydrosilane through a $\eta^1\text{-silane}$ complex, as studied by DFT calculations.

Keywords: fluxionality • hydrides • hydrosilylation • molybdenum • silicon

Introduction

Heavy elements of the platinum group catalyze a variety of important reduction reactions,^[1] such as hydrosilylation,^[2] hydrogenation, and transfer hydrogenation. However, these reactions suffer from the rising cost and toxicity of precious metal catalysts; as such, there is an increasing call for cheaper and environmentally benign alternatives. Although first-row transition metals and iron in particular^[3] are at the “front line” of current research,^[4–8] other metal systems have also shown promise.^[9–11] Molybdenum is attractive in this regard because of its low cost and low toxicity, highlighted by the fact that it is the only second-row metal found in biological systems.^[12]

We have recently reported catalytic hydrosilylation reactions mediated by octahedral complex $[(\text{ArN}=\text{)Mo}(\text{H})(\text{Cl})(\text{PMe}_3)_3]$ (**1**).^[11b,f] Mechanistic studies of the hydrosilylation of benzaldehyde suggest that the reaction begins with the dissociation of the phosphine group that was *trans* to the hydride and the formation of aldehyde adduct $[\textit{trans}\text{-}(\text{ArN}=\text{)Mo}(\text{H})(\text{C}(\text{O})\text{H})(\text{PMe}_3)_2]$ (**2**).

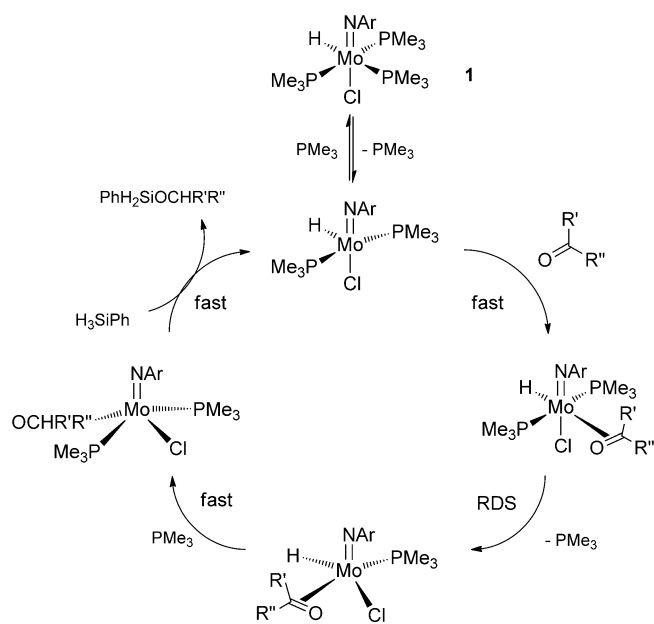
[a] Dr. A. Y. Khalimon, Dipl.-Ing. R. Simionescu, Dr. G. I. Nikonov
Chemistry Department, Brock University
500 Glenridge Avenue, St. Catharines, ON, L2S 3A1 (Canada)
E-mail: gnikonov@brocku.ca

[b] Prof. Dr. S. K. Ignatov, A. I. Okhupkin
Chemistry Department
N.I. Lobachevsky State University of Nizhny Novgorod
23 Gagarin Avenue, Nizhny Novgorod, 603950 (Russia)

[c] Prof. Dr. L. G. Kuzmina
N.S. Kurnakov Institute of General and Inorganic Chemistry
31 Leninskii Prospect, Moscow, 119991 (Russia)

[d] Prof. Dr. J. A. K. Howard
Chemistry Department, University of Durham
South Road, Durham, DH1 3LE (UK)

Supporting information for this article is available on the WWW under <http://dx.doi.org/10.1002/chem.201300376>, including procedures for the kinetic studies of complex **3**, parameters for the crystal structure determination, and full details of the EXSY NMR experiments and DFT calculations.



Scheme 1. Catalytic cycle for the hydrosilylation reaction mediated by complex **1**.

)Mo(H)(Cl)(PMe₃)₂(η²-O=CHPh)]. The rate-determining step (RDS) was found to be the rearrangement of the latter species into alkoxy intermediate [(ArN=)Mo(Cl)(PMe₃)₂(OCH₂Ph)] (Scheme 1). Then,

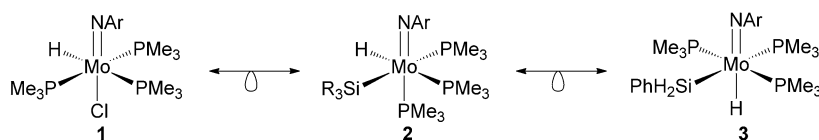
we hypothesized that compounds with the formula [(ArN=)Mo(H)(SiR₃)(PMe₃)₃] would be more active as catalysts because: 1) they would feature active hydride and silyl ligands; 2) they would have potentially labile phosphine ligands^[13] and, thus 3) they would meet the requirements for an active species in the classical mechanism of catalytic hydrosilylation, as suggested by Ojima and co-workers.^[14] We also believed that, as for related complex **1**, this molybdenum silyl hydride complex would have an octahedral geometry (**2**), with the silyl and hydride ligands located *trans* to the phosphine ligands. Such a ligand arrangement would place the ligands with the strongest *trans* influence (imido,^[15] silyl,^[16] and hydride)^[17] *trans* to each of the weakest ligands, in this case phosphine groups, thus optimizing the electronic properties of the complex.^[18] Our efforts to achieve this goal led to the preparation of complex **3**, which exhibited unusual structural features and dynamic behavior.^[19] Herein, we report a full account of this research, including catalytic and mechanistic studies.

Results and Discussion

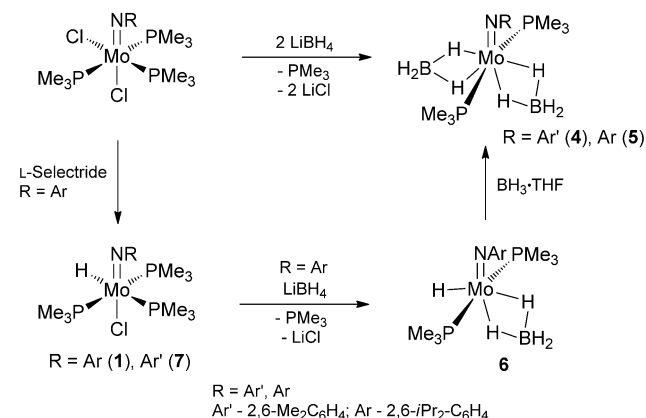
Precursor compounds: Although hypothetical complexes **2** and **3** only differ from complex **1** in the substitution of one

ligand (chloride), the preparation of these silyl complexes is not an easy task. The synthesis of silyl derivatives of complex **1** through a metathetical (salt elimination) route would require the use of stable silyl anions, which are limited to sterically encumbered species.^[20] We hypothesized that imido-supported (poly)hydride complexes may be more convenient precursors for a variety of species **2** and **3** through Mo–H/H–Si σ-bond metathesis or a H–H elimination/H–Si oxidative addition route (Scheme 1, Scheme 2).^[21] We have recently reported the preparation of borohydrides [(ArN=)Mo(η²-BH₄)₂(PMe₃)₂] (**4**) and [(ArN=)Mo(η²-BH₄)₂(PMe₃)₂] (**5**) as masked forms of imido hydride complexes, but these species happened to be very robust in their own right.^[22] To access more reactive precursors, we targeted the preparation of borohydride complexes of the type [(RN=)Mo(PMe₃)₂(H)(η²-BH₄)].

The addition of one equivalent of LiBH₄ to a solution of complex **1** in THF affords a highly fluxional and unstable complex, whose NMR features are consistent with mono-(borohydride) derivative [(ArN=)Mo(H)(η²-BH₄)(PMe₃)₂] (**6**, Scheme 3). At room temperature, ³¹P{¹H} NMR analysis of complex **6** shows a singlet at δ=3.2 ppm, which can be



Scheme 2. Possible silyl hydride analogues of catalyst **1**.



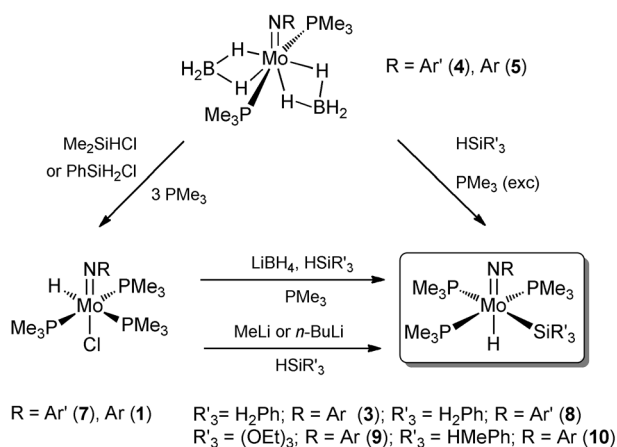
Scheme 3. Preparation and reactivity of Mo^{IV} borohydride complexes.

assigned to two equivalent phosphine groups. Fast exchange between the hydride and BH₄ ligands in complex **6** leads to a broad ¹H NMR signal at δ=−0.95 ppm, which integrates to 5H. All attempts to freeze out this exchange process by performing low temperature experiments on a 600 MHz NMR spectrometer only led to severe broadening of the spectra. Disappointingly, the instability of complex **6** hampered its full characterization.^[23] However, the addition of one equivalent of BH₃ to a freshly prepared sample of com-

plex **6** led to the clean formation of bis(borohydride) **5**, thus ensuring that we could reliably generate complex **6** in solution and use it as a precursor.

Imido-supported borohydride complexes are rare^[24,25] and Group 6 borohydride complexes are underrepresented in the literature.^[15b,26]

Preparation of silyl hydride complexes [(RN=)Mo-(SiR₃)(H)(PMe₃)₃] (R = Ar, Ar'): Borohydride complexes **4** and **5** turned out to be quite chemically robust, that is, they withstood an attempted abstraction of BH₃ by Lewis bases (NEt₃ or PMe₃) and, even more remarkably, did not react with equivalent amounts of an alcohol (ethanol or ethylene glycol) and water.^[22] Nevertheless, they did react, albeit very slowly, in the presence of silanes. Thus, the reactions of [(RN=)Mo(η²-BH₄)₂(PMe₃)₂] (**4**: R = Ar'; **5**: R = Ar) with chlorosilanes (Me₂SiHCl or PhSiH₂Cl) in the presence of three equivalents of PMe₃ resulted, after 3 days at ambient temperature, in the quantitative formation of the corresponding hydrido chloride complexes [(RN=)Mo(H)(Cl)(PMe₃)₃] (**2**: R = Ar; **7**: R = Ar'; Scheme 4).^[27] The



Scheme 4. Preparation of Mo^{IV} silyl hydride complexes **3**, **8–10**.

addition of less Lewis acidic hydrosilanes significantly slowed the reaction down, but they still led to the desired silyl hydride derivatives. Thus, the treatment of complexes **4** and **5** with PhSiH₃ in the presence of excess PMe₃ (3–5 equiv) led, after a few weeks at room temperature, to silyl hydride complexes [(RN=)Mo(H)(SiH₂Ph)(PMe₃)₃] (**8**: R = Ar'; **3**: R = Ar;^[19] Scheme 4). A more efficient way of preparing silyl hydride **3** involved reacting complex **2** with one equivalent of LiBH₄ and PhSiH₃ in the presence of PMe₃. It is very likely that this reaction proceeds through the intermediate formation of mono(borohydride) **6**, which then either undergoes Mo–H/H–Si metathesis followed by abstraction of the BH₃ group or initial BH₃ abstraction followed by the reaction with the silane.

The reaction of complex **5** with HSi(OEt)₃ and excess PMe₃ initially affords a metastable silyl derivative, [(ArN=)Mo(H)(Si(OEt)₃)(PMe₃)₃] (**9**, Scheme 4), which slowly

(over approximately one week in solution at RT) decomposes into a difficult-to-characterize mixture of products, the main component of which is tentatively suggested to be [(ArN=)Mo(OEt)₂(PMe₃)₃] (**11**) based on its NMR features.^[23]

Alternatively, the silyl hydride derivatives can be obtained by the reaction of complex **1** with RLi (R = Me or *n*Bu), followed by the addition of a hydrosilane (Scheme 4). Presumably, this reaction proceeds through the formation of an alkylhydride, [(ArN=)Mo(H)(R)(PMe₃)₃], which then undergoes the reductive elimination of the alkane, followed by oxidative addition of the hydrosilane. When R = Me, the formation of methane was confirmed by ¹H NMR spectroscopy.

Silyl hydride compounds **3** and **8–10**, as well as the new precursor complex [(ArN=)Mo(H)(Cl)(PMe₃)₃] (**7**), were characterized by multinuclear NMR and IR spectroscopy. The structure of complex **3** was also established by X-ray diffraction analysis. The spectroscopic features of complex **7** resemble those of previously reported complex **1**.^[11b]

¹H NMR spectra of silyl hydride derivatives **3** and **8–10** show the presence of hydride ligands, which appear as upfield-shifted signals at δ = −3.92 (dt, ²J(P,H) = 18.6 and 65.4 Hz), −3.56 (dt, ²J(H,P) = 18.5 and 65.4 Hz), −4.73 (dt, ²J(P,H) = 18.6 and 62.1 Hz), and −3.38 ppm (dt, ²J(H,P) = 20.1 and 68.1 Hz), respectively. In addition, the hydride substituents of isolated species **3** and **8** give rise to characteristic Mo–H stretches at 1699 and 1647 cm^{−1} in their IR spectra, respectively.

The silicon-bound protons in compounds **3**, **8**, and **10** afford downfield resonances at δ = 5.75 (t, ³J(H,P) = 7.8 Hz), 5.83 (t, ³J(H,P) = 7.8 Hz), and 5.78 ppm (br m), respectively. No Si–H coupling between the silicon nucleus and the Mo-bound hydride could be observed by ¹H NMR and ²⁹Si NMR spectroscopy, thus suggesting a classical silyl hydride structure.^[21,28] However, interestingly, the ¹J(Si,H) coupling constants (**3**: 147.0 Hz; **8**: 157.4 Hz; **10**: 143.1 Hz) are noticeably smaller compared to those in their parent silanes (180–200 Hz) and approach the values that were observed in some agostic Si–H⋯M complexes.^[28a] Although the smaller ¹J(Si,H) couplings may indicate some α-agostic Si–H⋯M interactions,^[29] the observation of normal Si–H stretches^[28a] in the IR spectra (**3**: 1998 cm^{−1}; **8**: 1998 cm^{−1}) is more consistent with the classical silyl description of these compounds. Our explanation of the relatively small ¹J(Si,H) coupling constant is that it may be the result of rehybridization of the silicon center: According to Bent's rule,^[30] the metal-bound silicon atom has more s-orbital character in the M–Si bond, thus leaving more p-character for bonding with more electronegative ligands, such as hydrides.^[28a] This effect diminishes the direct Si–H coupling to the Si-bound hydrides.

X-ray structure of complex [(ArN=)Mo(H)(SiH₂Ph)(PMe₃)₃] (3**) and DFT study of the model compounds:** The molecular structure of complex **3** presents several unexpected features: First, in contrast to the predicted geometry (**2**), two ligands with the strongest *trans* influence, that is, the hy-

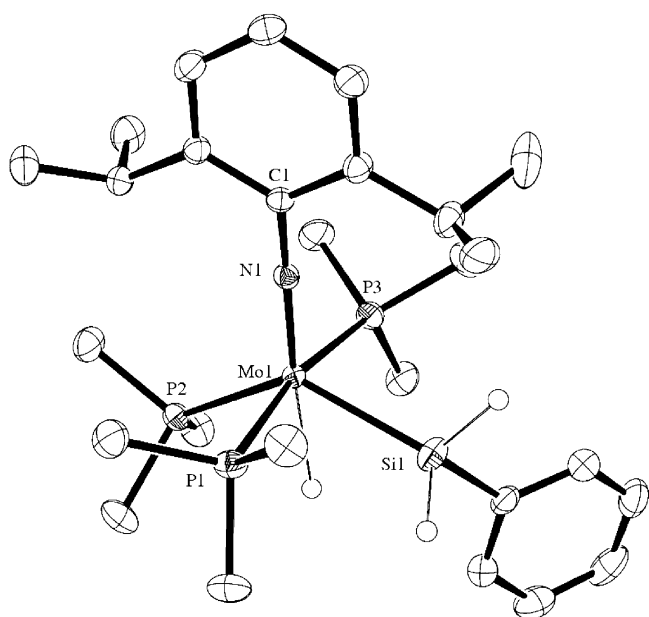


Figure 1. Molecular structure of complex **3**; hydrogen atoms, except for the hydride groups on the molybdenum and silicon atoms, are omitted for clarity.

hydride and imido ligands, are located *trans* to each other (Figure 1).^[31] In addition, such a ligand arrangement places the bulky PMe_3 and ArN groups *cis* to each other. Second, the length of the Mo-P bond (2.4699(5) Å) to the phosphine ligand that is *trans* to the silyl group is the same as those to the mutually *trans*-phosphines (2.4671(5) and 2.4861(5) Å). This observation is unexpected because silyl ligands usually exert a much stronger *trans* influence than the phosphine ligands.^[16] Such a surprising lack of *trans* influence can be explained by a significant deviation in the Si-Mo1-P2 bond angle (131.78(2)°) from the normal *trans* angle (180°). This distortion brings the silyl ligand closer to the hydride ligand; however, the resulting Si-H distance of 2.295 Å is still too long to suggest any significant bonding.^[28] The absence of silyl hydride interactions in the ground state of compound **3** is in accord with the spectroscopic data presented above.

To rationalize these unusual observations, a DFT study was performed. It was clear to us that the structural features of complex **3** were dictated by an interplay between steric and electronic factors and, therefore, that an exact modeling of the bulky NAr ligand may be required. On the other hand, we believed that the silyl group could be represented as SiH_2Me ; thus, the compound $[(\text{ArN}=\text{Mo})(\text{H})(\text{SiH}_2\text{Me})(\text{PMe}_3)_3]$ (**12**) appeared to be an adequate model for complex **3**. Four isomers of model compound **12** were studied. The calculated structure **12A** is very close to the X-ray determined structure of complex **3** (Table 1). To evaluate the steric and electronic effects in complex **3**, we also performed calculations on a truncated version of complex **12A**, the model complex $[(\text{PhN}=\text{Mo})(\text{H})(\text{SiH}_2\text{Me})(\text{PMe}_3)_3]$ (**13**). The main difference between structures **12A** and **13** is the removal of the *ortho*-isopropyl groups from complex **12**, which

Table 1. Selected bond lengths [Å] and angles [°] in compound **3** and in calculated models **12A–12D** and **13** (in parentheses).

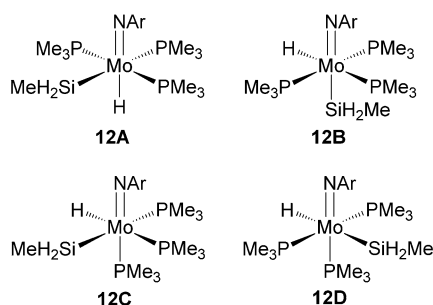
Bond	3	12A	12B	12C	12D
Mo–N	1.8081(16)	1.824 (1.811)	1.810	1.780	1.778
Mo–Si	2.5008(6)	2.538 (2.532)	2.722	2.577	2.592
Mo–H	1.9202	1.842 (1.850)	1.702	1.711	1.739
Mo–P	2.4862(5)	2.500 (2.496)	2.484	2.517	2.501
Mo–P	2.4669(5)	2.492 (2.487)	2.482	2.495	2.497
Mo–P(t) ^[a]	2.4699(5)	2.455 (2.435)	2.493	2.690 ^[b]	2.724 ^[b]
N–Mo–P(t)	119.66(5)	120.2 (117.3)			
N–Mo–X	108.24(5)	111.0 (109.3)			

[a] P(t) indicates the phosphine atom that is situated *trans* to ligand X (X = silyl or hydride). [b] PMe_3 group *trans* to the imido. [c] PMe_3 group *trans* to the silyl group.

results in somewhat shorter M=N and M-P bonds (Table 1), but the main structural features are retained, that is, the *trans*-to-silyl PMe_3 group and the SiH_2Ph group that both bend away from the imido ligand. Despite the significant difference in steric bulk, the resulting P-Mo-Si angle of 128.6° in structure **12A** is comparable with the P-Mo-Si angle of 133.4° in structure **13** (cf. the experimental value in complex **3**: 131.78(2)°). Therefore, we rationalize this distortion as being mainly electronic in nature: The *trans* PMe_3 and SiH_2Ph groups try to avoid the strong *trans* influence of the silyl ligand, so that the steric factor plays a secondary role.

Of the four calculated isomers of structure **12**, the most stable is **12A**, a close model of complex **3**. Next is isomer **12B** ($\Delta E = +1 \text{ kcal mol}^{-1}$), in which the silyl group is *trans* to the imido ligand. Such a ligand arrangement results in a shortening of the Mo=N bond (1.810 Å in **12B** versus 1.824 Å in **12A**, Table 1) and a significant lengthening of the Mo-Si bond to 2.722 Å, thus indicating a much stronger *trans* influence of the imido ligand versus the silyl group. Another noticeable feature is that the PMe_3 ligand that is located *trans* to the hydride group in structure **12B** stands farther away from the molybdenum atom (2.493 Å) than the phosphine group that is *trans* to the silyl group in structure **12A** (2.435 Å), whereas the bonds to the mutually *trans* phosphine groups remain almost the same. These trends indicate a stronger *trans* influence of the hydride ligand relative to the silyl group. This conclusion is elaborated further by comparing the Mo-P distances to the phosphine groups that are located *trans* to the imido, hydride, and silyl ligands in structure **12C** (2.690, 2.517, and 2.495 Å, respectively). Therefore, we conclude that the order of the *trans* influence in compounds **12A–12C** is imido > hydride > silyl.

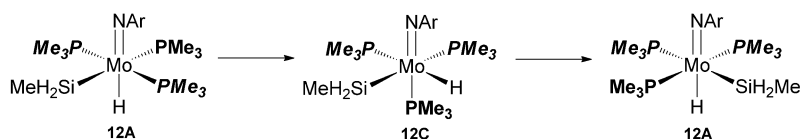
Finally, it is interesting to note that, of these four isomers of complex **12**, isomer **12C** is the least stable ($\Delta E = +7.4 \text{ kcal mol}^{-1}$). This result is unexpected because isomer **12C** is a model of our hypothetical complex **2**, which we anticipated to have the “optimized” *trans* influence. Inspection of the bond lengths in isomer **12C** shows that this species has the longest Mo-P bonds; thus, we hypothesize that it is the loss of a metal–phosphine interaction that destabilizes this isomer.



Fluxionality of $[(\text{ArN}=\text{Mo}(\text{H})(\text{SiH}_2\text{Ph})(\text{PMe}_3)_3]$ (3**):** ^{31}P - ^{31}P EXSY NMR showed that complex **3** underwent fast intramolecular exchange of the mutually *trans* phosphine groups with the unique phosphine that lies *trans* to the silyl group ($k_{\text{intra}}(22^\circ\text{C}) = (9.1 \pm 0.1) \times 10^{-2} \text{ s}^{-1}$). Although the fluxionality of octahedral complexes is not unknown, this is a relatively rare phenomenon and most fluxional octahedral complexes are found among polyhydride derivatives.^[32,33] Intensive studies into the fluxionality of octahedral complexes identified the Bailar-twist mechanism and related mechanisms as the principle pathways for intramolecular exchange.^[34] The Bailar-twist mechanism proceeds through a highly ordered trigonal prismatic transition state that is characterized by a negative entropy of activation.^[34b]

We have previously reported a positive (albeit small) entropy of activation for the intramolecular exchange process.^[19] However, our extensive DFT calculations of a potential exchange mechanism (see below) suggested that the entropy of activation should be negative. Therefore, we suspected that the higher temperature exchange data (at 55°C) could be compromised by the partial decomposition of the complex. Indeed, analysis of a temperature truncated data set (up to 45°C) affords a negative entropy of activation ($\Delta S^\ddagger_{\text{intra}} = -11.2 \text{ cal K}^{-1} \text{ mol}^{-1}$), in good accord with the calculations.

We explored two main possibilities for the intramolecular phosphine exchange: 1) The twist mechanism and 2) the formation of a fluxional pentacoordinate intermediate. Because complex **3** and its models **12A** and **13** are not homoleptic, the exchange of different PMe_3 groups is only possible as a result of at least two consecutive twists (Scheme 5). For our model compound **12A**, we succeeded in finding a transition state for the first step in Scheme 5 ($\Delta H^\ddagger = 19.1 \text{ kcal mol}^{-1}$, $\Delta G^\ddagger = 20.3 \text{ kcal mol}^{-1}$; Figure 2 left). As expected for a Bailar-like twist, this step is characterized by a negative entropy of activation ($\Delta S^\ddagger = -4.1 \text{ cal K}^{-1} \text{ mol}^{-1}$). The second



Scheme 5. Intramolecular phosphine exchange in complex **3** through two consecutive twists.

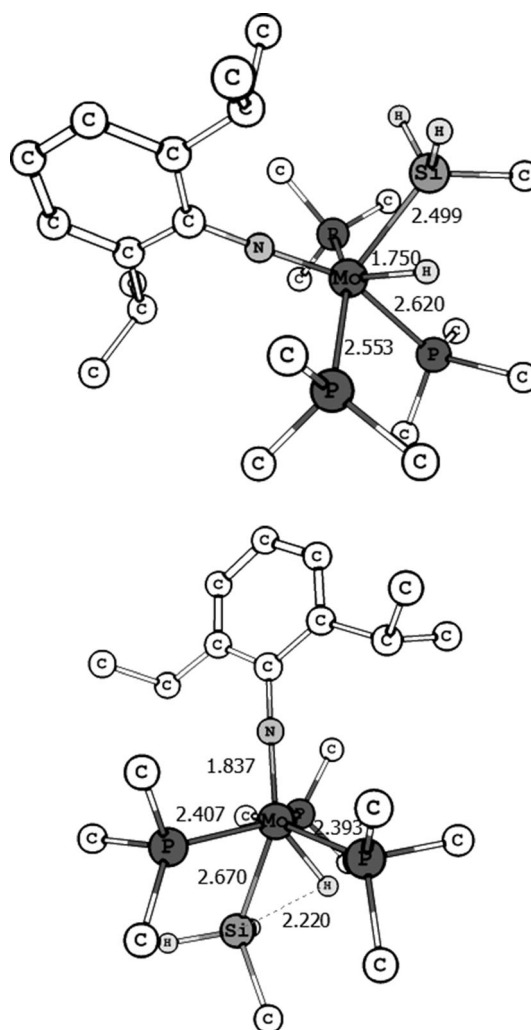
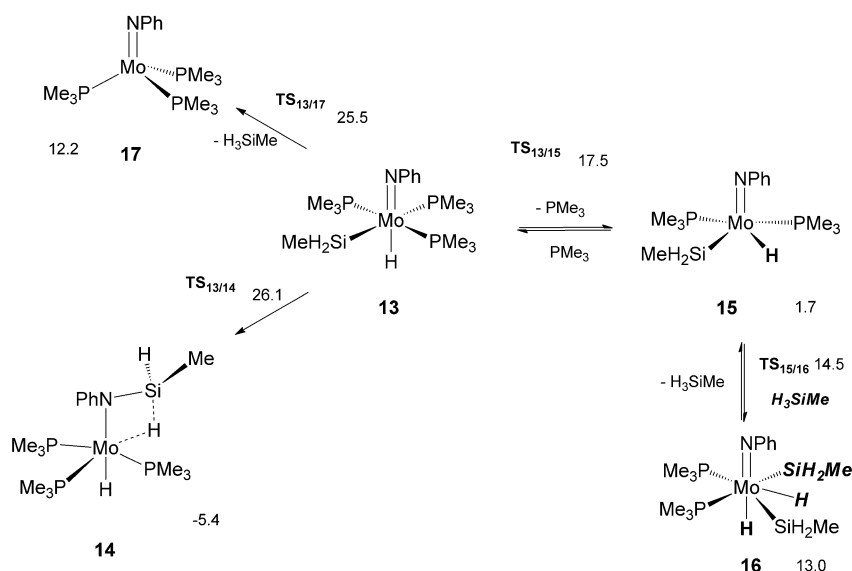


Figure 2. Transition states for intramolecular phosphine exchange in complex **12A**. Hydrogen atoms, apart from hydrides, are omitted for clarity. Top: Bailar-like twist; bottom: new, lower energy transition state.

step in Scheme 5 is just the reverse reaction of the first step and is characterized by a lower activation barrier ($\Delta H^\ddagger = 11.3 \text{ kcal mol}^{-1}$, $\Delta G^\ddagger = 13.5 \text{ kcal mol}^{-1}$, $\Delta S^\ddagger = -4.1 \text{ cal K}^{-1} \text{ mol}^{-1}$). The reaction parameters for the formation of intermediate **12C** (Scheme 5) are $\Delta_r H = 7.8 \text{ kcal mol}^{-1}$, $\Delta_r G = 6.8 \text{ kcal mol}^{-1}$, and $\Delta_r S = 3.5 \text{ cal K}^{-1} \text{ mol}^{-1}$.

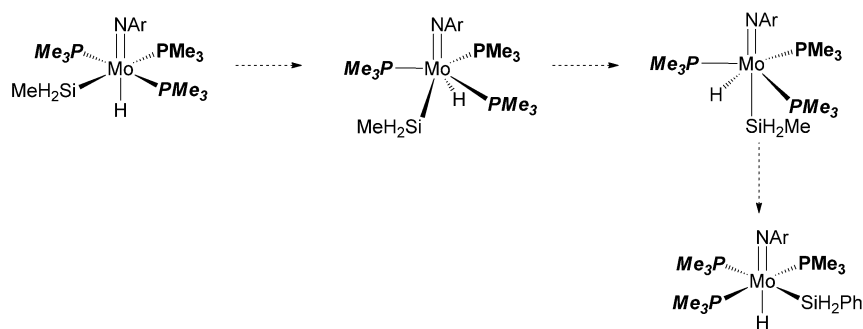
We considered two possibilities for the formation of a pentacoordinate intermediate from complex **3**: The first option was the migration of the silyl group onto the imido ligand to give a silylamido species.^[35] The possibility of such a process was investigated for the silyl migration in less sterically loaded model structure **13** (Scheme 6). However, the barrier for silyl migration ($26.1 \text{ kcal mol}^{-1}$) to give complex **14** (Scheme 6) was much larger than the barrier for phosphine dissociation from the same compound (17.5 kcal



Scheme 6. DFT calculated silyl migration and dissociation of PMe_3 and H_3SiPh from complex **13**. Free energies relative to complex **13** are given in kcal mol^{-1} .

mol^{-1}) to give complex **15**. Therefore, the imido/silylamido rearrangement in Scheme 6 does not lie on the reaction coordinate of the intramolecular phosphine exchange in complex **3**.

A thoughtful reviewer of our preliminary communication^[19] suggested that exchange in complex **3** may proceed through the formation of a pentacoordinate silane σ complex.^[21,28] We explored this possibility for model compound **12**, but failed to find a stable Mo^{II} silane intermediate. However, we found another transition state that corresponded to the process shown in Scheme 7. In this mechanism, the silyl



Scheme 7. Trajectory of intramolecular phosphine exchange in complex **12A**.

ligand moves closer to the hydride and, after passing under the Mo-P bond, pops up on another edge of the P_3 triangle. The net result is the exchange of two phosphine ligands. The silane ligand is not formed on this trajectory because the Si-H distance remains too long for significant bonding to occur (e.g., 2.220 Å in the transition state). The enthalpy and entropy of activation for such an unconventional mechanism are 15.1 kcal mol^{-1} and $-5.5 \text{ cal K}^{-1} \text{ mol}^{-1}$, respective-

ly, which are in good agreement with our corrected experimental values (19.1 kcal mol^{-1} and $-11.2 \text{ cal K}^{-1} \text{ mol}^{-1}$, respectively).^[36]

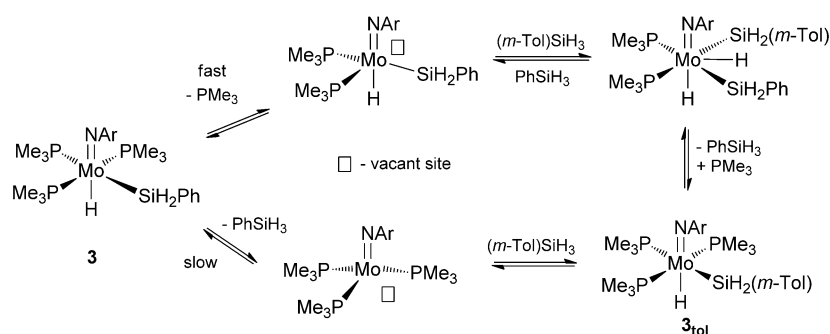
A ^{31}P - ^{31}P EXSY NMR study of a mixture of complex **3** and free PMe_3 also established the occurrence of an intermolecular phosphine exchange, although this process occurred at a slower rate ($k_{\text{inter}}(22^\circ\text{C}) = (1.82 \pm 0.08) \times 10^{-3} \text{ s}^{-1}$). The determination of the activation parameters revealed a dissociatively activated interchange ($\Delta S_{\text{inter}}^\ddagger = 30.9 \pm 10.6 \text{ cal K}^{-1} \text{ mol}^{-1}$, $\Delta H_{\text{inter}}^\ddagger = 30.3 \pm 3.4 \text{ kcal mol}^{-1}$, and $\Delta G_{\text{inter}}^\ddagger = 21.2 \pm 6.5 \text{ kcal mol}^{-1}$).

To our great surprise, we discovered that the addition of excess PhSiH_3 (about 10 equiv) to a mixture of complex **3** and PMe_3 facilitated the intermolecular exchange of PMe_3 ($\Delta G_{\text{inter}}^\ddagger = 20.5 \pm 7.7 \text{ kcal mol}^{-1}$, $\Delta H_{\text{inter}}^\ddagger = 23.9 \pm 4.0 \text{ kcal mol}^{-1}$, $\Delta S_{\text{inter}}^\ddagger = 11.7 \pm 12.4 \text{ cal K}^{-1} \text{ mol}^{-1}$, $k_{\text{inter}}(22^\circ\text{C}) = (4.0 \pm 0.04) \times 10^{-3} \text{ s}^{-1}$). It is well-established that an external nucleophile (X) can facilitate the dissociation of a ligand (Y) from an octahedral complex through a dissociatively activated X/Y interchange.^[32d] The typical nucleophiles for such an interchange are N-, O-, and S-based ligands. But, to the best of our knowledge, the participation of a nucleophile that lacks a lone pair of electrons (e.g., silane) in such an X/Y interchange has not previously been reported.

Silyl/silane exchange in $[(\text{ArN}=\text{Mo}(\text{H})(\text{SiH}_2\text{Ph})(\text{PMe}_3)_3)]$ (**3**):

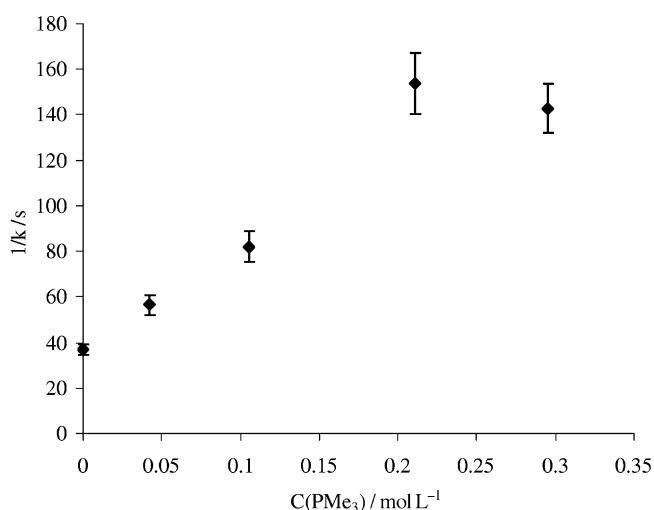
At slightly elevated temperatures ($>30^\circ\text{C}$), the ^1H EXSY NMR spectra of compound **3** show an exchange between the Si-bound protons of the SiH_2Ph ligand and those of the free silane, PhSiH_3 . The addition of (*m*-Tol) SiH_3 to a solution of complex **3** in C_6D_6 leads, after 10 min at room temperature, to 27% conversion into $[(\text{ArN}=\text{Mo}(\text{H})[\text{SiH}_2(\textit{m}\text{-Tol})](\text{PMe}_3)_3)]$ (**3_{tol}**, Scheme 8), thus confirming that the exchange process involves the actual exchange of silicon centers and not only the exchange of Si-bound hydrogen atoms. It is noteworthy that no exchange between the Mo-bound hydride and the SiH_2 hydrogen atoms of the silyl ligand or the free silane is observed on the EXSY timescale within the temperature range $30\text{--}50^\circ\text{C}$.^[37] This observation rules out Si-H dissociation as the main re-

ligand moves closer to the hydride and, after passing under the Mo-P bond, pops up on another edge of the P_3 triangle. The net result is the exchange of two phosphine ligands. The silane ligand is not formed on this trajectory because the Si-H distance remains too long for significant bonding to occur (e.g., 2.220 Å in the transition state). The enthalpy and entropy of activation for such an unconventional mechanism are 15.1 kcal mol^{-1} and $-5.5 \text{ cal K}^{-1} \text{ mol}^{-1}$, respective-

Scheme 8. Suggested mechanism for silyl/silane exchange in complex **3**.

action pathway for the silyl/silane exchange. However, the treatment of complex **3** with one equivalent of PhSiD_3 showed, after 10 min at room temperature, 59% and 65% of H/D scrambling at the MoH and SiH positions, respectively. Thus, this latter experiment suggests the possibility of elimination of the H–Si bond from complex **3**, albeit at a much slower rate than the silyl/silane exchange as observed by EXSY.

The activation parameters of the silyl/silane exchange in complex **3** were calculated by using 1D ^1H EXSY NMR spectroscopy through an initial-rate analysis.^[38] We found a positive entropy of activation ($\Delta S^\ddagger = 34.6 \pm 5.6 \text{ cal K}^{-1} \text{ mol}^{-1}$, $\Delta H^\ddagger = 31.0 \pm 1.7 \text{ kcal mol}^{-1}$, $\Delta G_{295}^\ddagger = 20.8 \pm 3.4 \text{ kcal mol}^{-1}$, $k(22^\circ\text{C}) = (2.7 \pm 0.1) \times 10^{-3} \text{ s}^{-1}$), which suggested the operation of a dissociatively activated process. Further insight into the mechanism comes from the observation that the rate of the silyl/silane exchange process depends on the concentration of added PMe_3 (Figure 3). At 35°C , the $1/k_{\text{eff}}$ parameter is proportional to the concentration of phosphine and exhibits a saturation behavior upon increasing the concentration of PMe_3 ($k_1(35^\circ\text{C}) = (6.7 \pm 0.9) \times 10^{-3} \text{ s}^{-1}$). These observations suggest that the dominant pathway for silyl/silane exchange

Figure 3. Dependence of the rate constant of silyl/silane exchange between complex **3** and PhSiH_3 at 30°C on the concentration of added PMe_3 .

involves the dissociation of a PMe_3 ligand. The calculated activation parameters for the exchange between complex **3** and PhSiH_3 in the presence of excess PMe_3 (about 7 equiv; a pseudo-first-order regime) revealed an even larger value of the entropy of activation, $\Delta S^\ddagger = 48.3 \pm 7.0 \text{ cal K}^{-1} \text{ mol}^{-1}$ ($\Delta H^\ddagger = 21.8 \pm 4.2 \text{ kcal mol}^{-1}$, $\Delta G_{295}^\ddagger = 36.0 \pm 2.2 \text{ kcal mol}^{-1}$), and a slower reaction rate ($k(22^\circ\text{C}) = (6.3 \pm 0.1) \times 10^{-4} \text{ s}^{-1}$ versus $k(22^\circ\text{C}) = (2.7 \pm 0.1) \times 10^{-3} \text{ s}^{-1}$ for the exchange without PMe_3). All of these observations can be accounted for by Scheme 6. The silyl/silane exchange occurs through two parallel pathways: 1) The predissociation of PMe_3 , the formation of unsaturated silyl hydride complex **15**, and the oxidative addition of silane to give bis(silyl) intermediate **16**, and 2) A much slower route that proceeds through the dissociation of PhSiH_3 to give tris(phosphine) complex **17**.

Density functional theory (DFT) calculations^[23] on the model system $[(\text{PhN}=\text{Mo}(\text{H})(\text{SiH}_2\text{Me})(\text{PMe}_3)_3)]$ (**13**) and MeSiH_3 further support this conclusion. The elimination of silane to give the tris(phosphine) compound $[(\text{PhN}=\text{Mo}(\text{PMe}_3)_3)]$ (**17**) occurs through transition state $\text{TS}_{13/17}$, which is $8.0 \text{ kcal mol}^{-1}$ higher than the barrier for phosphine dissociation to give the diphosphine silyl hydride complex $[(\text{PhN}=\text{Mo}(\text{H})(\text{SiH}_2\text{Me})(\text{PMe}_3)_2)]$ (**15**, Scheme 6). The addition of silane to the latter complex affords a bis(silyl) derivative of Mo^{VI} , $[(\text{PhN}=\text{Mo}(\text{H})_2(\text{SiH}_2\text{Me})_2(\text{PMe}_3)_2)]$ (**16**), which has a pentagonal bipyramidal structure, with the original Mo-bound hydride occupying an apical position and the hydride that stems from the oxidative addition of silane occupying the equatorial position between the silyl ligands. The elimination of a Si–H bond from complex **16** primarily takes place in the equatorial plane, which allows us to explain why the exchange process in complex **3** on the EXSY time-scale involves the silyl ligand but not the orthogonally positioned hydride ligand.

Hydride silyl complexes of Mo^{VI} are very rare and the first such species has only very recently been reported.^[11c] We found further experimental evidence for the feasibility of such an unusual Mo^{VI} bis(silyl) intermediate (**16**). Thus, an NMR-tube reaction of the complex $[\text{trans}-(\text{ArN}=\text{Mo}(\text{SiH}_2\text{Ph})(\text{O}i\text{Pr})(\text{PMe}_3)_2)]$ (**18**, see below) with excess PhSiH_3 at -45°C showed the fast formation of $[(\text{ArN}=\text{Mo}(\text{H})_2(\text{SiH}_2\text{Ph})_2(\text{PMe}_3)_2)]$ (**19**) as a mixture with the hydrosilylation products $\text{PhH}_2\text{Si}(\text{O}i\text{Pr})$ and $\text{PhHSi}(\text{O}i\text{Pr})_2$.

Catalytic reactivity of $[(\text{ArN}=\text{Mo}(\text{H})(\text{SiH}_2\text{Ph})(\text{PMe}_3)_3]$ (3**):** As mentioned in the Introduction, the initial design of complex **3** was driven by the desire to eliminate the rate-determining step in the hydrosilylation reactions catalyzed by complex **1**. Indeed, silyl hydride complex **3** was found to be a much better catalyst than hydrido chloride **1** (Table 2). For

Table 2. Hydrosilylation of organic substrates catalyzed by complex **3**.^[a]

Entry	Substrate	Silane	Product ^[b]	Conditions	Conversion [%]	Yield [%] ^[c]	TON ^[d]
1	PhC(O)H	PhSiH ₃	PhSiH ₂ (OCH ₂ Ph) PhSiH(OCH ₂ Ph) ₂	15 min, RT	100	47 53	20
2	PhC(O)H	PhMeSiH ₃	MePhHSi(OCH ₂ Ph)	18 h, RT	100	100	20
3	PhC(O)H	(EtO) ₃ SiH	(EtO) ₃ Si(OCH ₂ Ph) (EtO) ₂ Si(OCH ₂ Ph) ₂ (EtO)Si(OCH ₂ Ph) ₃	18 h, RT	100	41 29 30	20
4	PhC(O)Me	PhSiH ₃	PhSiH ₂ OCH(Me)Ph PhSiH(OCH(Me)Ph) ₂ PhCH ₂ CH ₃	2 days, RT/1 day, 50 °C	94	45 33 16	18.8
5	acetone	PhSiH ₃	PhH ₂ Si(OiPr) PhHSi(OiPr) ₂	3.4 h, RT	90	73 17	18
6		PMHS ^[e]	poly(methylisopropoxysiloxane)	3.9 h, RT 21 h, RT	58 82	58 82	11.6 16.4
7	1-hexene	PhSiH ₃	C ₆ H ₁₃ SiH ₂ Ph hexene-2 hexane	2 days, RT	27	5 1 21	5.4
8	EtOH	PhSiH ₃	PhH ₂ Si(OEt) PhHSi(OEt) ₂	20 min, RT	100	67 33	20
9	PhCN	PhSiH ₃	PhH ₂ Si(N=CHPh)	19.7 h, RT 41.9 h, RT	20 32	20 32	4 6.4
10	MeCN	PhSiH ₃	EtN(SiH ₂ Ph) ₂	20 min, RT	6	6	1.2

[a] Conditions: C₆D₆, [substrate]=0.06 M, 5.0 mol % of complex **3** (except for entries 4 and 7, in which 1 mol % was used). [b] Reactions with PhSiH₃ also gave Ph₂SiH₂, SiH₄, PhH₂Si–SiH₂Ph, and H₂ as by-products, which were produced by the catalytic redistribution and coupling of PhSiH₃. Increasing the temperature of the reaction increased the amount of the by-products. [c] All of the yields were determined by NMR analysis by using tetramethylsilane as an internal standard. [d] PMHS = poly(methylhydrosiloxane). TON = turnover number.

example, the hydrosilylation of benzaldehyde by PhSiH₃ catalyzed by compound **1**^[11a] requires 3 h at 50 °C, whereas the complex **3** catalyzed reaction takes only 15 min at room temperature (Table 2).

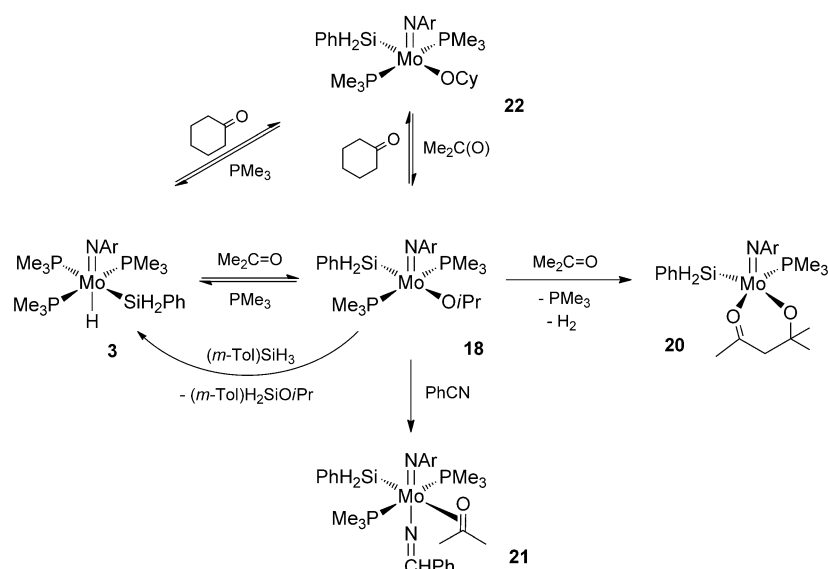
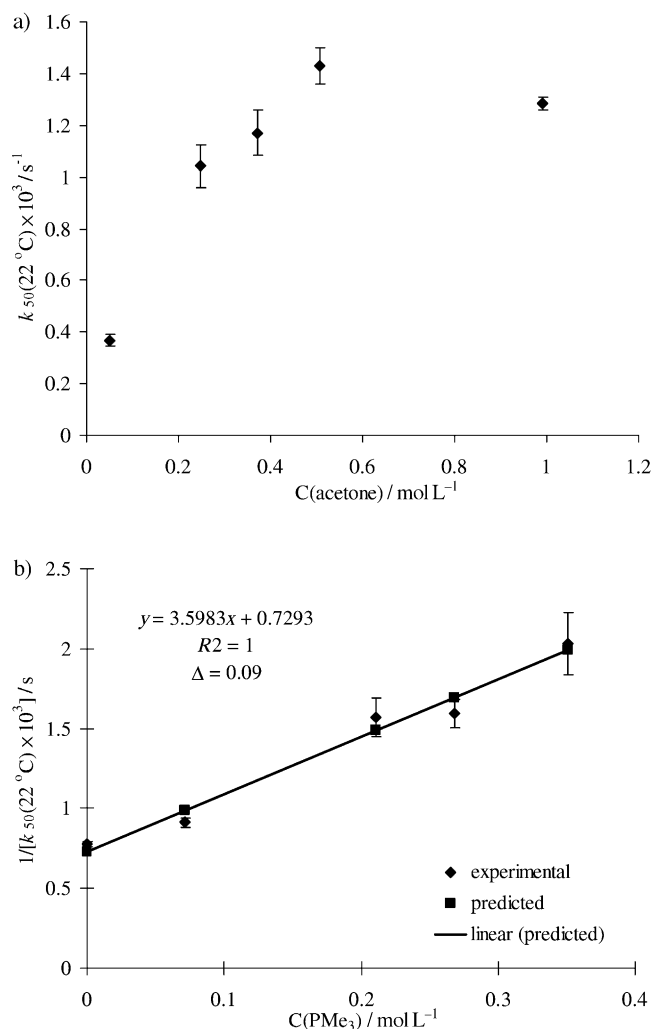
The reactions of benzaldehyde with PhSiH₃, PhMeSiH₂, and (EtO)₃SiH in the presence of 5 mol % of complex **3** all give 100 % conversion of the substrate in 15 min to 18 h at room temperature (Table 2, entries 1–3). A similar trend, with high yields of the hydrosilylation products, has also been observed for the complex **3** catalyzed addition of PhSiH₃ to acetophenone and acetone (Table 2, entries 4 and 5, respectively). Increasing the reaction time and temperature lead to silane redistribution^[39] and to the reduction of some carbonyl compounds to alkanes.^[40] The substitution of phenylsilane for the cheaper silane poly(methylhydrosiloxane) (PMHS) leads to a significantly decreased activity of complex **3**, thus affording, after 3.9 h at room temperature, only 58 % of the hydrosilylated product (Table 2, entry 6).

On the other hand, the activity of silyl complex **3** in the hydrosilylation of nitriles (acetonitrile and benzonitrile) was similar to that of chloride catalyst **1**. In particular, the reaction of MeCN with PhSiH₃ in the presence of 5 mol % of complex **3** only resulted, after 20 min at room temperature, in the stoichiometric formation of EtN(SiH₂Ph)₂ (6%; Table 2, entry 10). No further conversion of acetonitrile was observed over 24 h. At the same time, the hydrosilylation of benzonitrile selectively gives the mono(addition) product PhH₂SiN=CHPh in 20 % yield (Table 2, entry 9). Catalytic mono(hydrosilylation) of nitriles into imines has only been observed in a few cases.^[11a,b,e,f,41–43]

Experimental study of the mechanism of the hydrosilylation

of carbonyl compounds catalyzed by complex 3: In an attempt to understand the mechanism of the catalytic hydrosilylation of carbonyl compounds, stoichiometric reactions of complex **3** were studied. The addition of a few equivalents of PhSiH₃ to complex **3** only results in relatively slow silane redistribution and coupling to yield Ph₂SiH₂, SiH₄, and PhH₂Si–SiH₂Ph. In contrast, the addition of one equivalent of acetone to complex **3** results in carbonyl insertion into the Mo–H bond to give an equilibrium mixture of [*trans*-(ArN=)Mo(SiH₂Ph)(OiPr)(PMe₃)₂] (**18**), the starting complex **3**, and acetone (Scheme 9). The treatment of complex **3** with 5 equiv of Me₂C=O shifts the equilibrium towards complex **18**, thus showing almost complete conversion of the starting material after 30 min at room temperature. Longer reaction times (up to 12 h) and/or higher concentrations of acetone lead to a further reaction, thus affording the acetone-coupling product [(ArN=)Mo(SiH₂Ph)(κ²-O-C(Me)₂-CH₂C(O)Me)(PMe₃)] (**20**, Scheme 9).^[44]

At high concentrations of acetone, the reaction obeys pseudo-first-order kinetics ($k_1^{50}(22\text{ °C}) = (1.29 \pm 0.21) \times 10^{-3} \text{ s}^{-1}$; Figure 4a). Furthermore, in the pseudo-first-order regime (20-fold excess of acetone), $1/k_{\text{eff}}$ is proportional to the concentration of added PMe₃ (Figure 4b), which indicates that dissociation of the phosphine group is the first step in the reaction. Activation parameters for the reaction between complex **3** and excess acetone (about 20 equiv; a pseudo-first-order regime) were determined by kinetic VT NMR experiments.^[45] The positive entropy of activation indicates a dissociative mechanism ($\Delta S^\ddagger = 26.1 \pm 12.0 \text{ cal K}^{-1} \text{ mol}^{-1}$, $\Delta H^\ddagger = 30.0 \pm 3.5 \text{ kcal mol}^{-1}$, $\Delta G^\ddagger^{295} = 21.3 \pm 7.1 \text{ kcal mol}^{-1}$), which is consistent with the kinetic NMR studies. Therefore, we suggest that the reaction of

Scheme 9. Reactions of complex **3** with ketones and benzonitrile.Figure 4. a) Dependence of the rate constant for the reaction of complex **3** with acetone at 22 °C on the concentration of acetone. b) Dependence of the rate constant for the reaction of complex **3** with acetone (20 equiv) at 22 °C on the concentration of PMe₃.

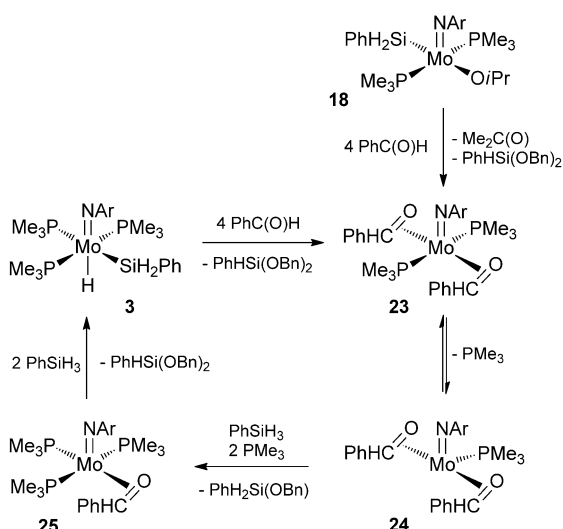
complex **3** with acetone proceeds through the rate-limiting dissociation of phosphine, followed by fast coordination of the carbonyl group and C=O insertion into the Mo–H bond.

The addition of excess PMe₃ to a mixture of complexes **3** and **18** does not result in the anticipated elimination of the Si–O bond, as suggested by the classical Ojima's mechanism of hydrosilylation.^[14] Rather, the phosphine addition merely shifts the equilibrium towards complex **3**, thus establishing the β-CH activation in the OiPr ligand. Such a reversible carbonyl insertion into an early-transition-metal–hydride bond is very rare,^[46] because alkoxides that are ligated to electro-

positive early metals usually defy CH activation. β-CH activation in the alkoxide ligand was further confirmed by the treatment of complex **18** with one equivalent of benzonitrile, which resulted in the fast transfer hydrogenation of the nitrile and the quantitative formation of the benzylidenamide derivative, [(ArN=)Mo(SiH₂Ph)(N=CHPh)(η²-O=CMe₂)(PMe₃)₂] (**21**, Scheme 9), as a mixture of two isomers.^[11e,47,48] Analogous transfer hydrogenation was observed in the reaction of complex **18** with cyclohexanone, thereby resulting in a mixture of the starting material and [trans-(ArN=)Mo(SiH₂Ph)(OCy)(PMe₃)₂] (**22**). This latter species can be prepared independently by the reaction of complex **3** with cyclohexanone (Scheme 9).

Even more surprisingly, the addition of a different silane, *m*-TolSiH₃, to complex **18** results in the quantitative regeneration of complex **3**, with the complete retention of the SiH₂Ph group (Scheme 9). Therefore, the silyl ligand in complex **3** plays the unusual role of a spectator ligand, which is at odds with the classical Ojima mechanism of hydrosilylation.^[14]

In contrast to the reaction with acetone, the treatment of complex **3** with excess PhHC=O (about 4 equiv and more) leads, after 5 min at room temperature, to the elimination of the hydrosilylation product, PhHSi(OBn)₂,^[11a,e,49] and to the formation of bis(aldehyde) complex [trans-(ArN=)Mo(η²-PhHC=O)₂(PMe₃)₂] (**23**, Scheme 10).^[50] The product is highly fluxional, even at –20 °C. However, the ³¹P{¹H} NMR spectrum at –60 °C shows two doublets (²J(P,P) = 218.7 Hz) at δ = 8.0 and 6.4 ppm for two nonequivalent *trans*-PMe₃ ligands. In the ¹H NMR spectrum, the carbonyl protons of two η²-benzaldehyde ligands appear as broad, upfield-shifted signals at δ = 5.42 (br s) and 5.18 ppm (br d, J(H,P) = 9.6 Hz),^[51] that are coupled in the ¹H–¹³C HSQC spectrum to the carbonyl carbon atoms at δ = 85.2 and 86.1 ppm, respectively.



Scheme 10. Preparation and reactivity of bis(benzaldehyde) complex **23**.

Increasing the temperature to -40°C resulted in the dissociation of one PMe_3 group and the formation of the mono(phosphine) derivative $[(\text{ArN}=\text{Mo}(\eta^2\text{-PhHC}=\text{O})_2(\text{PMe}_3)]$ (**24**, Scheme 10), which was characterized by IR and multinuclear NMR spectroscopy and by X-ray diffraction (Figure 5). The compound is fluxional in the presence of PMe_3 and the ^{31}P - ^{31}P EXSY NMR spectra revealed an exchange between complex **23**, complex **24**, and PMe_3 , even at -30°C . The ^1H NMR spectrum of complex **24** shows two nonequivalent upfield-shifted $\text{HC}=\text{O}$ signals at $\delta=5.77$ and 3.33 ppm, which are coupled in the ^1H - ^{13}C HSQC NMR spectrum to the carbonyl carbon atoms at $\delta=74.8$ and 84.0 ppm, respectively. The formulation of complex **24** as an η^2 adduct is further supported by the appearance of red-

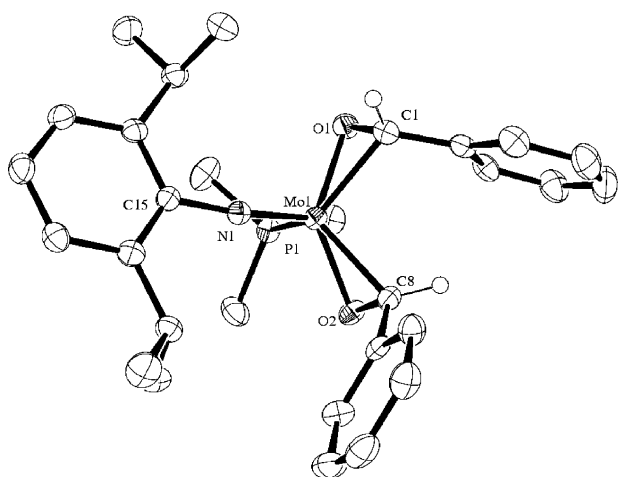


Figure 5. Molecular structure of complex **24**; anisotropic displacement parameters are plotted at 50% probability. Hydrogen atoms, except for CHO atoms, are omitted for clarity. Selected bond lengths [\AA] and angles [$^{\circ}$]: Mo1-N1 1.743(2), Mo1-O1 1.9862(18), Mo1-O2 2.0012(18), Mo1-C1 2.131(3), Mo1-C8 2.126(3), Mo1-P1 2.5250(7), O1-C1 1.371(3), O2-C8 1.376(3); Mo1-N1-C15 166.51(18), O1-Mo1-C1 38.71(9), O2-Mo1-C8 38.79(8), O1-C1-Mo1 94.92(13), O2-C8-Mo1 65.68(13), Mo1-O1-C1 76.37(13), Mo1-O2-C8 75.53(13), N1-Mo1-P1 103.34(7).

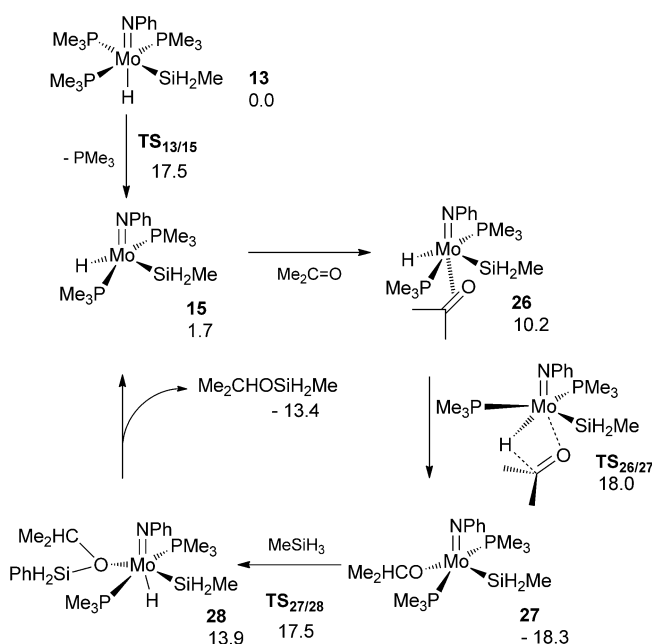
shifted $\text{C}=\text{O}$ stretches in the IR spectrum (1596 and 1487 cm^{-1} versus 1720 cm^{-1} for the free $\text{PhHC}=\text{O}$).^[11a-c,e,50,51] Complex **24** is unstable under vacuum; however, cooling the reaction mixture down to -30°C allowed us to crystallize complex **24** in its analytically pure form. Alternatively, a mixture of complexes **23** and **24** can be obtained through a transfer hydrogenation reaction of benzaldehyde with isopropoxy derivative **18** (Scheme 10).

Complex **24** has a distorted trigonal pyramidal geometry (Figure 5), in which the imido ligand is located at the apical position and two benzaldehyde ligands and a phosphine group form the base. The Mo1-N1-C15 angle ($166.51(18)^{\circ}$) is close to linear, thus suggesting that the imido ligand acts as a $6e$ donor to the metal, which stabilizes the $16e$ valence shell.^[52] The short $\text{Mo}-\text{C}$ distances ($2.131(3)$ and $2.126(3)\text{ \AA}$) indicate significant back donation from the molybdenum atom to the $\text{C}=\text{O}$ π^* orbital, so that the bonding approaches the metalaoxacyclopropane limit,^[53] consistent with the presence of a Mo^{VI} center. The $\text{Mo}-\text{O}$ (O1 : $1.9862(18)$ and O2 : $2.0012(18)\text{ \AA}$) and $\text{Mo}-\text{C}$ distances for two benzaldehyde ligands are slightly different, which reflects the difference in their coordination: One benzaldehyde group has its phenyl ring pointing towards the imide, whereas the other benzaldehyde has its Ph group directed away from the imide. Interestingly, the $\text{Mo}-\text{P1}$ bond ($2.5250(7)\text{ \AA}$) is significantly elongated compared with those in complex **3** ($2.4671(5)$, $2.4699(5)$, and $2.4861(5)\text{ \AA}$), despite the fact that complex **24** appears to be less sterically strained. One possible explanation for this difference could be that the presence of two carbon centers that are effectively *trans* to the phosphine group.

The treatment of complex **24** with one equivalent of PhSiH_3 in the presence of two equivalents of PMe_3 at -15°C results in the hydrosilylation of one of the benzaldehyde ligands^[11a,e,49] and the formation of $[(\text{ArN}=\text{Mo}(\eta^2\text{-PhHC}=\text{O})(\text{PMe}_3)_3)]$ (**25**, Scheme 10). The subsequent addition of excess silane at 0°C cleanly regenerates complex **3** and releases $\text{PhH}_2\text{Si}(\text{OBn})$.^[11a,e,49] In the absence of PMe_3 , complex **25** slowly reacts with PhSiH_3 at 5°C to give complex **3**, toluene (which stems from complete reduction of $\text{PhHC}=\text{O}$), and some other unidentified Mo products.

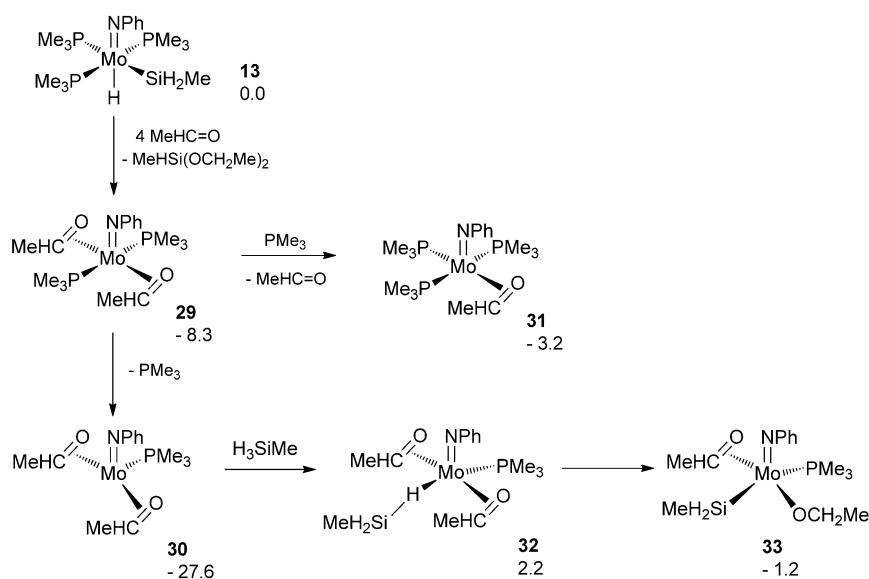
DFT study of the mechanism of hydrosilylation catalyzed by complex 3: To shed more light on the hydrosilylation mechanism, a DFT study was carried out for the model system $[(\text{PhN}=\text{Mo}(\text{H})(\text{SiH}_2\text{Me})(\text{PMe}_3)_3)]$ (**13**). The coordination of acetone to diphosphine intermediate **14** gives high-energy adduct **26** (Scheme 11). Carbonyl insertion into the $\text{Mo}-\text{H}$ bond gives alkoxy complex **27**, as a model of complex **18**. Complex **27** undergoes the heterolytic splitting of silane by the $\text{Mo}-\text{O}$ bond^[11b-d,f] through the rate-determining transition state $\text{TS}_{27/28}$ to give silyl ether adduct **28**, which readily dissociates (with a barrier of 2.2 kcal mol^{-1}) the product $\text{MeH}_2\text{Si}(\text{O}i\text{Pr})$ and regenerates catalyst **15**.

DFT calculations were also performed for the model system $\text{13/MeC}(\text{O})\text{H/MeSiH}_3$. The formation of the bis-(aldehyde) complex $[\textit{trans}-(\text{PhN}=\text{Mo}(\eta^2\text{-MeC}(\text{O})\text{H})_2-$



Scheme 11. DFT-calculated mechanism for the hydrosilylation of acetone catalyzed by complex **13**. Free energies relative to complex **13** are given in kcal mol⁻¹.

(PMe₃)₂] (**29**, Scheme 12), as a model of compound **23**, is profitable by 8.3 kcal mol⁻¹. The dissociation of phosphine from complex **29** to give the mono(phosphine) derivative [(PhN=)Mo(η^2 -MeC(O)H)₂(PMe₃)] (**30**) stabilizes the system by a further 19.3 kcal mol⁻¹, whereas substitution of the aldehyde in complex **29** for a phosphine group affords the tris(phosphine) complex [(PhN=)Mo(η^2 -MeC(O)H)(PMe₃)₃] (**31**), which is 5.1 kcal mol⁻¹ less stable than complex **29**. The addition of silane to complex **30** leads to the η^1 -silane intermediate [(PhN=)M(η^1 -H-SiH₂Me)(η^2 -



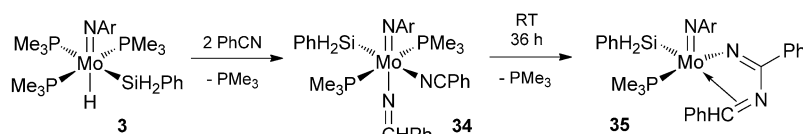
Scheme 12. A possible mechanism of the hydrosilylation of MeC(O)H by **13**. Free energies relative to complex **13** are given in kcal mol⁻¹.

MeC(O)H)₂(PMe₃)] (**32**), which then rearranges into the silyl alkoxy derivative [(PhN=)Mo(SiH₂Me)(OCH₂Me)(η^2 -MeC(O)H)(PMe₃)] (**33**, Scheme 12). This latter complex is analogous to bis(phosphine) complex **27** (Scheme 11) and, thus, can react with silanes to furnish the silyl ether product. Although the tris(phosphine) benzaldehyde adduct (see **31** in Scheme 12, as a model of real complex **25**) is a stable species, its intermediacy in the true catalytic cycle is questionable, owing to the presence of large excesses of the aldehyde and the silane.

Reaction of complex 3 with a nitrile: In attempt to better understand the complex **3** catalyzed hydrosilylation of nitriles, the stoichiometric reaction of complex **3** with benzonitrile was studied. The addition of two equivalents of PhCN affords, after 1 h at room temperature, the product of nitrile insertion into the Mo–H bond,^[11e,47,48] [(ArN=)Mo(SiH₂Ph)(N=CHPh)(NCPH)(PMe₃)₂] (**34**, Scheme 13). The ¹H NMR spectrum of complex **34** revealed an approximate 1:1 mixture of isomers (*cis* and *trans* with respect to the aldimine ligand). The resonances for the aldimine CHPh protons, at δ = 7.93 (t, *J*(H,P) = 6.6 Hz) and 8.50 ppm (t, *J*(H,P) = 7.2 Hz), respectively, are coupled in the ¹H–¹³C HSQC NMR spectrum to the aldimine carbon atoms at δ = 153.0 and 197.1 ppm. The ³¹P{¹H} NMR spectrum of complex **34** gives rise to two singlets at δ = 2.3 and 2.8 ppm (one for each isomer), thus indicating an equivalency and, hence, a *trans* arrangement of the PMe₃ groups.

Complex **34** was found to be metastable in solution and decomposed through PMe₃ dissociation to cleanly afford the coupling product [(ArN)Mo(κ^3 -N=C(Ph)–N=CHPh)(PMe₃)] (**35**, Scheme 13). This latter species can be formed, for example, through the intramolecular nucleophilic addition of the benzylidenamide ligand (N=CHPh) at the unsaturated carbon atom of the coordinated benzonitrile.^[54] The

¹H NMR spectrum of complex **35** shows a upfield-shifted resonance of the methylenamide fragment, N=CHPh,^[47,49] at δ = 5.28 ppm (s), which is coupled in the ¹H–¹³C HSQC NMR spectrum to the upfield ¹³C NMR signal at δ = 54.7 ppm. The quaternary methylenamide carbon atom affords a resonance at δ = 197.1 ppm in the ¹³C NMR spectrum. Such a significant upfield shift of the signals that are due to the methylenamide proton and the carbon atoms of complex **35** suggests a κ^3 -coordination mode of the N=C(Ph)–N=CHPh ligand, for example, through the presence of additional π coordination of the N=C(Ph)–N=CHPh moiety.^[55]



Scheme 13. Reactivity of complex **3** towards benzonitrile.

Conclusion

We have prepared a series of new imido-supported silyl hydride complexes of Mo^{IV} and established their stoichiometric and catalytic reactivity patterns. Silyl complex [(ArN=)Mo(H)(SiH₂Ph)(PMe₃)₃] (**3**) showed a much improved catalytic activity in the hydrosilylation of carbonyl compounds than the previously reported chloro derivative [(ArN=)Mo(H)(Cl)(PMe₃)₃] (**1**). X-ray diffraction analysis of compound **3** showed an unusual geometry that defied the usual rules of *trans* influence. Complex **3** is involved in three types of fluxional behavior: 1) intramolecular exchange of phosphine ligands; 2) exchange with free phosphine groups; and 3) silyl/silane exchange. A DFT study of the intramolecular phosphine exchange revealed a low-energy pathway that was different to the common Bailar-twist mechanism. The intermolecular phosphine exchange proceeds through a dissociative mechanism, according to kinetic and DFT studies. The interesting new aspect is that the phosphine dissociation is facilitated by the free silane, which constitutes the first example of a dissociatively activated substitution in which the incoming nucleophile lacks a lone pair of electrons. The silyl/silane exchange proceeds through a phosphine-dissociation/silane-addition pathway to give a rare bis(silyl)-dihydride complex of Mo^{VI} (**19**). This species was observed by low temperature NMR spectroscopy and its existence was supported by DFT calculations (**16**, Scheme 6). A study of the stoichiometric reactivity of complex **3** with acetone and benzaldehyde revealed unexpected features of the mechanism of hydrosilylation reactions. In the case of acetone, the hydrosilylation reaction proceeded through an intermediate silyl alkoxy complex, [*trans*-(ArN=)Mo(SiH₂Ph)(O*i*Pr)(PMe₃)₂] (**18**). Complex **18** does not undergo the elimination of a Si–O bond, as predicted by the conventional Ojima mechanism of hydrosilylation. Rather, complex **18** presents a rare case of the β-CH activation of an alkoxide ligand in an early-metal complex. Therefore, the silyl ligand plays the unusual role of a spectator ligand. For the hydrosilylation of benzaldehyde, the reaction proceeds through the formation of a new bis(benzaldehyde) complex, [(ArN=)Mo(η²-PhC(O)H)₂(PMe₃)₃] (**24**). DFT calculations of the model system [(PhN=)Mo(η²-MeC(O)H)₂(PMe₃)₃] (**30**) suggest that the hydrosilylation reaction proceeds through the η¹ addition of silane MeSiH₃ and the formation of silyl alkoxy derivative [(PhN=)Mo(η²-MeC(O)H)(SiH₂Me)(OCH₂Me)(PMe₃)₃] (**33**).

Experimental Section

General: All manipulations were carried out under an inert atmosphere in a glove-box and by using conventional Schlenk techniques. Dry Et₂O, toluene, hexanes, and MeCN were obtained by using Grubbs-type purification columns; other solvents were dried by

distillation from appropriate drying agents. NMR spectra were recorded on Bruker DPX-300 and Bruker DPX-600 instruments (¹H: 300 and 600 MHz, ¹³C: 75.5 and 151 MHz, ²⁹Si: 59.6 and 119.2 MHz, ³¹P: 121.5 and 243 MHz, respectively). NMR analysis was performed at RT unless specified. IR spectra were recorded on a Perkin–Elmer 1600 FTIR spectrometer. Elemental analysis was performed at ANALEST (University of Toronto). The preparations of [(RN=)Mo(Cl)₂(PMe₃)₃] (R = Ar', Ar),^[56] [(RN=)Mo(η²-BH₄)₂(PMe₃)₂] (**4**: R = Ar'; **5**: Ar),^[22a] and [(ArN=)Mo(H)(Cl)(PMe₃)₃] (**1**)^[11b] have been reported previously. PhSiCl₃, HSi(OEt)₃, PhMeSiCl₂, tetramethylsilane (TMS), PMHS, PMe₃, PhC(O)H, PhC(O)Me, acetone, 1-hexene, PhCN, MeCN, LiBH₄, LiAlD₄, and (*m*-Tol)MgCl were purchased from Aldrich. PhSiH₃, PhSiD₃, and PhMeSiH₂ were prepared from their corresponding chlorosilanes by treatment with LiAlH₄/LiAlD₄. (*m*-Tol)SiH₃ was prepared according to a literature procedure from SiCl₄ and (*m*-Tol)MgCl.^[57] All of the catalytic reactions, NMR-scale reactions, and kinetic experiments were performed under a nitrogen atmosphere by using J. Young NMR tubes that were equipped with Teflon valves. The structures and yields of all of the hydrosilylated products were determined by NMR spectroscopy by using tetramethylsilane as an internal standard.

NMR-scale reaction of [(Ar'N=)Mo(η²-BH₄)₂(PMe₃)₂] (4**) with Me₂SiHCl:** PMe₃ (17.0 μL, 0.17 mmol) and Me₂SiHCl (7.0 μL, 0.06 mmol) were added at RT to a solution of complex **4** (21.8 mg, 0.06 mmol) in C₆D₆ (0.6 mL) in an NMR tube. The reaction mixture was left to stand at RT for 3 days until complete conversion of the starting material had been observed. NMR analysis showed the selective formation of [(Ar'N=)Mo(H)(Cl)(PMe₃)₃] (**7**). After extraction with hexanes and drying under vacuum, the product was isolated in its analytically pure form. Yield: 23.1 mg, 88%; ¹H NMR (300 MHz, C₆D₆): δ = 1.35 (d, ²J(H,P) = 5.7 Hz, 9H; PMe₃), 1.43 (vt, ²J(H,P) = 6.0 Hz, 18H; 2PMe₃), 2.39 (s, 6H; 2CH₃, Ar'N), 5.38 (dt, ²J(H,P) = 51.3 Hz, ²J(H,P) = 29.4 Hz, 1H; MoH), 6.79 ppm (m, 3H; *p*-H and *m*-H, Ar'N); ¹³C{¹H} NMR (75.5 MHz, C₆D₆): δ = 20.0 (s; CH₃, Ar'N), 21.1 (vt, ¹J(C,P) = 11.1 Hz; PMe₃), 21.4 (d, ¹J(C,P) = 15.1 Hz; PMe₃), 123.7 (s; *p*-C, Ar'N), 127.9 (s; *m*-C, Ar'N), 133.0 ppm (s; *o*-C, Ar'N), 153.9 ppm (s; *i*-C, Ar'N); ³¹P{¹H} NMR (121.5 MHz, C₆D₆): δ = -1.6 (d, ²J(P,P) = 14.6 Hz; 2PMe₃), -17.1 ppm (t, ²J(P,P) = 14.6 Hz; PMe₃); IR (nujol): $\tilde{\nu}$ = 1713 cm⁻¹ (s; Mo-H).

Preparation of (ArN=)Mo(H)(SiH₂Ph)(PMe₃)₃ (3**):** *Method A:* PhSiH₃ (132.0 μL, 1.07 mmol) was added to a solution of [(ArN=)Mo(η²-BH₄)₂(PMe₃)₂] (**5**, 486.0 mg, 1.07 mmol) and PMe₃ (0.22 mL, 2.14 mmol) in toluene (50 mL) at RT. The reaction mixture was stirred for 7 days at RT. Then, all of the volatile compounds were removed by evaporation and the residue was dried and extracted with Et₂O (30 mL). The solution in Et₂O was concentrated and left to stand at -78 °C overnight to give complex **3** as a yellow powder, which was dried under vacuum. Yield: 152.0 mg, 23%.

Method B: NMR-scale reaction: A 1.6 M solution of MeLi in Et₂O (22.0 μL, 0.04 mmol) was added to a mixture of PhSiH₃ (6.5 μL, 0.05 mmol) and [(ArN=)Mo(H)(Cl)(PMe₃)₃] (**1**, 19.0 mg, 0.04 mmol) in C₆D₆ (0.6 mL) at RT in an NMR tube. The reaction mixture was left to stand at RT for 10 min and the formation of white precipitate of LiCl was observed. NMR analysis showed the quantitative formation of complex **3**.

Method C: A solution of PhSiH₃ (128.0 μL, 1.04 mmol), PMe₃ (108.0 μL, 1.04 mmol), and complex **2** (111.0 mg, 0.21 mmol) in benzene (10 mL) was added through a cannula into a 2.0 M solution of LiBH₄ in THF (104.0 μL, 0.21 mmol) at RT. The reaction mixture was allowed to stir for 30 min. During this time, the color turned from brown to yellow and the

formation of a white precipitate of LiCl was observed. The mixture was filtered, all of the volatile compounds were removed by evaporation, and the residue was extracted with hexanes (50 mL). The solution was concentrated to about 10 mL and the product was crystallized at -30°C overnight to give complex **3** as a fine yellow solid (109.7 mg, 87% yield). ^1H NMR (600 MHz, C_6D_6): $\delta = -3.92$ (dt, $^2J(\text{P,H}) = 18.6$ Hz, $^2J(\text{P,H}) = 65.4$ Hz, 1H; MoH), 1.17 (br s, 18H; 2PMe₃), 1.21 (d, $^2J(\text{H,P}) = 6.6$ Hz, 9H; MoH), 1.31 (d, $^3J(\text{H,H}) = 6.6$ Hz, 12H; 4CH₃, ArN), 4.39 (sept, $^3J(\text{H,H}) = 6.6$ Hz, 2H; 2CH, ArN), 5.75 (t+sat, $^3J(\text{H,P}) = 7.8$ Hz, $^3J(\text{H,Si}) = 147.0$ Hz, 2H; SiH₂), 7.01 (d, $^3J(\text{H,H}) = 7.2$ Hz, 2H; *m*-H, ArN), 7.05 (m, $^3J(\text{H,H}) = 7.2$ Hz, 1H; *p*-H, ArN), 7.19 (t, $^3J(\text{H,H}) = 7.2$ Hz, 1H; *p*-H, PhSi), 7.28 (t, $^3J(\text{H,H}) = 7.2$ Hz, 2H; *m*-H, PhSi), 8.08 ppm (d, $^3J(\text{H,H}) = 7.2$ Hz, 2H; *o*-H, PhSi); $^{13}\text{C}\{^1\text{H}\}$ NMR (151 MHz, C_6D_6): $\delta = 21.4$ (vt, $^1J(\text{C,P}) = 22.6$ Hz; 2PMe₃), 24.2 (s; 4CH₃, ArN), 25.2 (d, $^1J(\text{C,P}) = 22.6$ Hz; PMe₃), 26.4 (s; 2CH, ArN), 122.9 (s; *p*-C, ArN), 123.3 (s; *m*-C, ArN), 126.7 (s; *p*-C, PhSi), 127.1 (s; *m*-C, PhSi), 132.0 (s; *i*-C, PhSi), 136.6 (s; *o*-C, PhSi), 145.4 (s; *o*-C, ArN), 146.6 ppm (s; *i*-C, ArN); $^{31}\text{P}\{^1\text{H}\}$ NMR (243 MHz, C_6D_6): $\delta = -1.9$ (d, $^2J(\text{P,P}) = 23.8$ Hz; 2PMe₃), 10.0 ppm (t, $^2J(\text{P,P}) = 23.8$ Hz; PMe₃); ^{31}P NMR (selectively decoupled from methyl groups, 243 MHz, C_6D_6): $\delta = -1.9$ (br m; 2PMe₃), 10.0 ppm (dt, $^2J(\text{H,P}) = 65.5$ Hz, $^2J(\text{P,P}) = 23.8$ Hz; PMe₃); $^{29}\text{Si}\{^1\text{H}\}$ NMR (119.2 MHz, C_6D_6): $\delta = 0.2$ ppm (td, $^2J(\text{Si,P}) = 9.6$ Hz, $^2J(\text{Si,P}) = 21.7$ Hz; SiH₂Ph); IR (nujol): $\tilde{\nu} = 1699$ (s; Mo–H), 1998 cm^{-1} (s; Si–H); elemental analysis calcd (%) for C₂₇H₃₂MoNP₂Si (607.655): C 53.37, H 8.63, N 2.31; found: C 53.76, H 8.53, N 2.21.

Preparation of [(ArN=)Mo(H)(SiH₂Ph)(PMe₃)₃] (8): PhSiH₃ (58.8 μL , 0.476 mmol) and PMe₃ (150.0 μL , 1.428 mmol) were added in one portion to a solution of complex **4** (189.0 mg, 0.476 mmol) in toluene (50 mL) at RT. No visual change in the mixture was observed and the mixture was stirred at RT for 2 weeks. All of the volatile compounds were removed by evaporation and the residue was dried under vacuum and extracted with Et₂O (30 mL). Then, the solution was concentrated to 5 mL, an equal amount of hexanes was added, and the mixture was left to stand at -30°C , overnight, to give complex **8** a fine yellow powder, which was dried under vacuum. Yield: 125.5 mg, 48%; ^1H NMR (600 MHz, C_6D_6): $\delta = -3.56$ (dt, $^2J(\text{P,H}) = 18.5$ Hz, $^2J(\text{P,H}) = 65.4$ Hz, 1H; MoH), 1.12 (vt, $^2J(\text{H,P}) = 6.5$ Hz, 18H; 2PMe₃), 1.20 (d, $^2J(\text{H,P}) = 6.5$ Hz, 9H; PMe₃), 2.49 (s, 6H; 2CH₃, ArN), 5.83 (t, $^3J(\text{H,P}) = 7.8$ Hz, 2H; SiH₂), 6.89 (t, $^3J(\text{H,H}) = 7.5$ Hz, 1H; *p*-H, ArN), 6.95 (d, $^3J(\text{H,H}) = 7.5$ Hz, 2H; *m*-H, ArN), 7.18 (t, $^3J(\text{H,H}) = 7.5$ Hz, 1H; *p*-H, PhSi), 7.28 (t, $^3J(\text{H,H}) = 7.5$ Hz, 2H; *m*-H, PhSi), 8.09 ppm (d, $^3J(\text{H,H}) = 7.5$ Hz, 2H; *o*-H, PhSi); $^{13}\text{C}\{^1\text{H}\}$ NMR (75.5 MHz, C_6D_6): $\delta = 20.9$ (s; CH₃, ArN), 21.6 (vt, $^1J(\text{C,P}) = 21.9$ Hz; PMe₃), 25.6 (d, $^1J(\text{C,P}) = 21.9$ Hz; PMe₃), 123.6 (s; *p*-C, ArN), 126.9 (s; *p*-C, PhSi), 127.1 (s; *m*-C, ArN), 128.3 (s; *m*-C, PhSi), 135.3 (s; *o*-C, ArN), 136.8 (s; *o*-C, PhSi), 148.7 (s; *i*-C, PhSi), 156.4 ppm (s; *i*-C, ArN); $^{31}\text{P}\{^1\text{H}\}$ NMR (121.5 MHz, C_6D_6): $\delta = -1.5$ (d, $^2J(\text{P,P}) = 23.1$ Hz; 2PMe₃), 10.5 ppm (t, $^2J(\text{P,P}) = 23.1$ Hz; PMe₃). ^{29}Si INEPT+ NMR (59.6 MHz, $J = 200$ Hz, C_6D_6): $\delta = 1.7$ ppm (t, $^1J(\text{Si,H}) = 157.4$ Hz; SiH₂Ph); IR (nujol): $\tilde{\nu} = 1647$ (s; Mo–H), 2152 cm^{-1} (s; Si–H); elemental analysis calcd (%) for C₂₃H₄₄MoNP₂Si (551.549): C 50.09, H 8.04, N 2.54; found: C 50.54, H 7.98, N 2.73.

Reaction of [(ArN=)Mo(η^2 -BH₄)₂(PMe₃)₂] (5) with HSi(OEt)₃: (EtO)₃SiH (0.24 mL, 1.28 mmol) and PMe₃ (0.33 mL, 3.21 mmol) were added in one portion to a solution of complex **5** (0.15 g, 0.32 mmol) in Et₂O (20 mL) at RT. The reaction mixture was stirred at RT for 5 days. All of the volatile compounds were removed by evaporation to give [(ArN=)Mo(H)(Si(OEt)₃)(PMe₃)₃] (**9**) as a brown oil, which was dried under vacuum. Yield: 72.2 mg, 34%. The product was unstable at RT in solution and slowly (1 week) decomposed to form [(ArN=)Mo(OEt)₂(PMe₃)₃] (**11**) and a mixture of unknown products. All attempts to isolate compound **7** in its analytically pure form failed, owing to its decomposition.

Complex 9: ^1H NMR (300 MHz, C_6D_6): $\delta = -4.73$ (dt, $^2J(\text{P,H}) = 18.6$ Hz, $^2J(\text{P,H}) = 62.1$ Hz, 1H; MoH), 1.20 (d, $^2J(\text{H,P}) = 6.6$ Hz, 9H; PMe₃), 1.31 (d, $^3J(\text{H,H}) = 6.9$ Hz, 12H; 4CH₃, NAr), 1.39 (t, $^3J(\text{H,H}) = 6.9$ Hz, 9H; 3CH₃, Si(OEt)₃), 1.46 (vt, $^2J(\text{H,P}) = 6.6$ Hz, 18H; 2PMe₃), 4.02 (q, $^3J(\text{H,H}) = 6.9$ Hz, 6H; 3CH₂, Si(OEt)₃), 4.43 (sept, $^3J(\text{H,H}) = 6.9$ Hz, 2H; 2CH, NAr), 6.95–6.97 ppm (m, 3H; *m*-H and *p*-H, NAr); $^{31}\text{P}\{^1\text{H}\}$ NMR

(121.5 MHz, C_6D_6): $\delta = 10.8$ (t, $^2J(\text{P,P}) = 24.3$ Hz, 1P; PMe₃), -1.46 ppm (d, $^2J(\text{P,P}) = 24.3$ Hz, 2P; 2PMe₃); $^{13}\text{C}\{^1\text{H}\}$ NMR (75.5 MHz, C_6D_6): $\delta = 146.1$ (s; *i*-C, NAr), 124.9 (s; *o*-C, NAr), 123.6 (s; *m*-C, NAr), 123.0 (s; *p*-C, NAr), 58.1 (s; CH₂, Si(OEt)₃), 26.5 (s; CH, NAr), 25.2 (d, $^1J(\text{C,P}) = 23.4$ Hz; PMe₃), 24.9 (s; CH₃, NAr), 23.0 (vt, $^1J(\text{C,P}) = 21.1$ Hz; PMe₃), 19.7 ppm (s; CH₃, Si(OEt)₃); ^1H - ^{29}Si HSQC NMR (f1 = 600 MHz, f2 = 119.2 MHz, $J = 7$ Hz, C_6D_6 , ^{29}Si projection): $\delta = 25.6$ ppm (Si(OEt)₃).

Complex 11: ^1H NMR (300 MHz, C_6D_6): $\delta = 6.86$ – 7.04 (m, 3H; *m*-H and *p*-H, NAr), 4.00 (m, 6H; 2CH, NAr and 2CH₂, Mo(OEt)₂), 1.39 (vt, $^2J(\text{H,P}) = 7.2$ Hz, 18H; 2PMe₃), 1.27 (d, $^2J(\text{H,P}) = 7.8$ Hz, 9H; PMe₃), 1.21 (t, $^3J(\text{H,H}) = 6.9$ Hz, 6H; 2CH₃, Mo(OEt)₂), 1.14 ppm (d, $^3J(\text{H,H}) = 6.9$ Hz, 12H; 4CH₃, NAr); $^{31}\text{P}\{^1\text{H}\}$ NMR (121.5 MHz, C_6D_6): $\delta = 2.6$ (t, $^2J(\text{P,P}) = 34.0$ Hz, 1P; PMe₃), -8.84 ppm (d, $^2J(\text{P,P}) = 34.0$ Hz, 2P; 2PMe₃); $^{13}\text{C}\{^1\text{H}\}$ NMR (75.5 MHz, C_6D_6): $\delta = 147.2$ (s; *i*-C, NAr), 132.6 (s; *o*-C, NAr), 123.4 (s; *m*-C, NAr), 119.2 (s; *p*-C, NAr), 59.6 (s; CH₂, Mo(OEt)₂), 27.5 (s; CH, NAr), 25.8 (s; CH₃, Mo(OEt)₂), 23.4 (d, $^1J(\text{C,P}) = 24.9$ Hz; PMe₃), 22.9 (s; CH₃, NAr), 17.4 ppm (vt, $^1J(\text{C,P}) = 22.6$ Hz; PMe₃).

Preparation of [(ArN=)Mo(H)(SiHMePh)(PMe₃)₃] (10): A 1.6 M solution of *n*BuLi in hexanes (0.33 mmol) was added to a mixture of PhMeSiH₂ (67.0 μL , 0.49 mmol) and complex **1** (174.0 mg, 0.33 mmol) in benzene (10 mL) at RT. The mixture was stirred at ambient temperature for 30 min. The formation of a white precipitate of LiCl was observed. All of the volatile compounds were removed by evaporation and the residue was extracted with hexanes (15 mL). The solvent was removed under reduced pressure to give a dark-brown oil. Recrystallization from hexanes at -80°C yielded complex **10** as a dark-brown solid. Yield: 15.6 mg, 8%. The product was formed as a mixture of isomers, owing to chirality at the silicon center. ^1H NMR (300 MHz, C_6D_6): $\delta = 7.93$ (d, $^3J(\text{H,H}) = 6.9$ Hz, 2H; *o*-H, SiPh), 7.30 (t, $^3J(\text{H,H}) = 7.2$ Hz, 2H), 6.98–7.20 (m, 4H), 5.78 (br m, 1H; SiH), 4.27 (sept, $^3J(\text{H,H}) = 6.9$ Hz, 2H; 2CH, NAr), 1.27 (m, $^3J(\text{H,H}) = 6.9$ Hz, $^2J(\text{H,P}) = 6.3$ Hz, 21H; 12H from 4CH₃, NAr and 9H from PMe₃), 1.21 (d, $^2J(\text{H,P}) = 6.6$ Hz, 9H; PMe₃), 1.14 (d, $^3J(\text{H,H}) = 4.5$ Hz, 3H; SiMe), 1.04 (d, $^2J(\text{H,P}) = 6.0$ Hz, 9H; PMe₃), -3.38 ppm (dt, $^2J(\text{H,P}) = 68.1$ Hz and 20.1 Hz; MoH); $^{13}\text{C}\{^1\text{H}\}$ NMR (75.5 MHz, C_6D_6): $\delta = 21.8$ (d, $^1J(\text{C,P}) = 19.6$ Hz; PMe₃), 23.1 (d, $^1J(\text{C,P}) = 15.8$ Hz; PMe₃), 24.80 (s; 4CH₃, NAr), 24.83 (s; 4CH₃, NAr), 26.65 (d, $^1J(\text{C,P}) = 23.4$ Hz; PMe₃), 26.73 (d, $^1J(\text{C,P}) = 21.9$ Hz; PMe₃), 27.3 (s; 2CH, NAr), 123.9 (s; *m*-C, NAr), 124.9 (s; *p*-C, NAr), 126.8 (s; *p*-C, SiPh), 127.5 (s; *m*-C, SiPh), 129.9 (s; *i*-C, SiPh), 135.0 (s; *o*-C, NAr), 136.1 (s; *o*-C, SiPh), 145.3 ppm (s; *i*-C, NAr); $^{31}\text{P}\{^1\text{H}\}$ NMR (121.5 MHz, C_6D_6): $\delta = -2.6$ (qd, $^2J(\text{P,P}) = 29.2$ Hz, 23.1 Hz, 21.9 Hz, 23.1 Hz, 2P; 2PMe₃), 11.9 ppm (dd, $^2J(\text{P,P}) = 23.1$ Hz and 21.9 Hz, 1P; PMe₃); ^{29}Si INEPT+ NMR (59.6 MHz, $J = 200$ Hz, C_6D_6): $\delta = 13.0$ ppm (d, $^1J(\text{Si,H}) = 143.1$ Hz; SiHMePh).

Reaction of [(ArN=)Mo(H)(Cl)(PMe₃)₃] (1) with LiBH₄: A 2.0 M solution of LiBH₄ in THF (0.10 mL, 0.09 mmol; Important: BH₃ should not be present!) was added in one portion to a solution of complex **1** (50.0 mg, 0.09 mmol) in Et₂O (10 mL) at RT. The reaction mixture was stirred at RT for 45 min. NMR analysis showed the formation of a mixture of [(ArN=)Mo(H)(η^2 -BH₄)(PMe₃)₂] (**6**, highly fluxional at RT) and unidentified decomposition products. All attempts to isolate complex **6** in its analytically pure form were unsuccessful. The addition of BH₃/THF to complex **6** gave complex **5**. ^1H NMR (300 MHz, C_6D_6): $\delta = 7.02$ (t, $^3J(\text{H,H}) = 7.8$ Hz, 1H; *p*-H, NAr), 6.89 (d, $^3J(\text{H,H}) = 7.8$ Hz, 2H; *m*-H, NAr), 4.41 (sept, $^3J(\text{H,H}) = 6.9$ Hz, 2H; 2CH, NAr), 1.18 (d, $^3J(\text{H,H}) = 6.9$ Hz, 12H; 4CH₃, NAr), 0.90 ppm (br s, 18H; 2PMe₃); $^{31}\text{P}\{^1\text{H}\}$ NMR (121.5 MHz, C_6D_6): $\delta = 3.3$ ppm (s; PMe₃).

NMR-scale reaction of complex 3 with PhSiD₃: PhSiD₃ (2.1 μL , 0.017 mmol) was added in one portion to a solution of complex **3** (10.3 mg, 0.017 mmol) and TMS (1.0 μL , 0.007 mmol) in C_6D_6 (0.6 mL) at RT in an NMR tube. The reaction mixture was left to stand at RT for 10 min. NMR analysis showed deuterium scrambling at the silyl and hydride positions: 59% and 65% H/D exchange were observed for the hydride and silyl positions of complex **3**, respectively. The percentage of incorporated D was calculated by integration of the residual H resonances for the hydride and silyl substituents of the complex before and after the addition of PhSiD₃. In both cases, all of the integrals were normalized to the integral for TMS.

NMR-scale reaction of complex 3 with (*m*-Tol)SiH₃: (*m*-Tol)SiH₃ (2.5 μL, 0.017 mmol) was added in one portion to a solution of complex 3 (10.3 mg, 0.017 mmol) and TMS (1.0 μL, 0.007 mmol) in C₆D₆ (0.6 mL) at RT in an NMR tube. The reaction mixture was left to stand at RT for 10 min. NMR analysis showed the formation of a mixture of complexes 3 (73%) and 3_{tot} (27%). The relative compositions of complexes 3 and 3_{tot} were calculated by integration of the *o*-H signals of the SiPh and Si(*m*-Tol) groups (by correlation of the SiH protons and the *o*-H protons of the Ph and *m*-Tol groups with the *i*-C atom of the Ph and *m*-Tol groups in the ¹H-¹³C HMBC NMR spectra) in these complexes and normalization of these integrals to the intensity of the TMS resonance.

Reaction of complex 3 with PhC(O)H: Method A: RT NMR-scale reaction: PhC(O)H (11.6 μL, 0.114 mmol) was added in one portion to a solution of complex 3 (17.4 mg, 0.029 mmol) in C₆D₆ (0.6 mL) at RT in an NMR tube. The reaction mixture was left at RT for 5 min. NMR analysis showed the complete conversion of the starting material and the quantitative formation of [(ArN=)Mo(η²-PhC(O)H)₂(PMe₃)₂] (23). The formation of PhHSi(OBn)₂ and the release of PMe₃ were also detected by NMR spectroscopy. Complex 23 was stable in solution at RT; however, decomposition was observed upon the removal of the volatile compounds under vacuum. ¹H-¹H EXSY NMR experiments on a mixture of complex 23 and PhC(O)H revealed no intermolecular benzaldehyde exchange, but some slow intramolecular benzaldehyde exchange was observed.

Method B: Low-temperature VT NMR-scale reaction: PhC(O)H (13.7 μL, 0.135 mmol) was added in one portion into a solution of complex 3 (20.5 mg, 0.0337 mmol) in [D₈]toluene (0.6 mL) that was frozen in liquid N₂ in an NMR tube. The mixture was slowly warmed to -30°C and placed into a precooled NMR machine at -30°C. The temperature was cooled to -50°C. At this temperature, NMR analysis showed the disappearance of complex 3 and the formation of complex 23 and PhHSi(OBn)₂. Warming the reaction mixture to -40°C led to the dissociation of PMe₃ and the formation of [(ArN=)Mo(η²-PhC(O)H)₂(PMe₃)₂] (24), which, according to ³¹P-³¹P EXSY NMR spectroscopy, underwent PMe₃ exchange with an external phosphine group and the PMe₃ ligands of compound 23. After the complete conversion of the starting material into complex 24 (about 2 h at -20°C), the reaction mixture was frozen in liquid N₂ and PhSiH₃ (12.5 μL, 0.1013 mmol) was added to the NMR tube. The sample was brought to -60°C and the mixture was gradually warmed with monitoring by NMR spectroscopy. At -15°C, NMR analysis showed the slow formation of [(ArN=)Mo(η²-PhC(O)H)(PMe₃)₃] (25) and PhH₂Si(OBn). At 0°C and higher, complex 25 reacted with PhSiH₃ to recover the starting compound (3) and form PhH₂Si(OBn). The addition of excess PhC(O)H to the mixture of complex 3, PhH₂Si(OBn), and PhHSi(OBn)₂ led, after leaving overnight at RT, to the formation of PhSi(OBn)₃. All attempts to isolate complex 25 were unsuccessful, owing to its instability.

Method C: PhC(O)H (30.0 μL, 0.295 mmol) was added in one portion to a solution of complex 3 (43.7 mg, 0.072 mmol) in Et₂O (2.5 mL) at RT. The reaction mixture was stirred at RT for 15 min and then kept at -30°C for 2 days, thereby affording yellow/orange crystals of complex 24, which were washed with cold (-30°C) hexanes and dried under vacuum. Yield: 19.7 mg, 49%.

Complex 23: ¹H NMR (600 MHz, [D₈]toluene, -55°C): δ = 0.66 (br s, 9H; PMe₃), 1.15 (br s, 9H; PMe₃), 1.23 (br m, 6H; 2CH₃, NAr), 1.29 (br s, 3H; CH₃, NAr), 1.45 (br s, 3H; CH₃, NAr), 3.47 (br s, 1H; CH, NAr), 4.36 (br s, 1H; CH, NAr), 5.18 (d, ³J(H,H) = 9.6 Hz, 1H; η²-O=CH), 5.42 (br s, 1H; η²-O=CH), 6.83–7.32 (m, 5H; *m*-H and *p*-H of NAr, *p*-H of two η²-O=CPh ligands (resonances are obscured by the signals of C₆D₆), PhSiH(OBn)₂), 7.40 (br s, 2H; *m*-H, η²-O=CPh), 7.47 (br s, 2H; *m*-H; η²-O=CPh), 7.71 (br d, ³J(H,H) = 6.0 Hz, 2H; *o*-H, η²-O=CPh), 7.96 ppm (br d, ³J(H,H) = 6.6 Hz, 2H; *o*-H, η²-O=CPh); ³¹P{¹H} NMR (243 MHz, [D₈]toluene, -27°C): δ = -7.0 (d, ²J(P,P) = 218.7 Hz; PMe₃), 7.4 ppm (d, ²J(P,P) = 218.7 Hz; PMe₃); ³¹P{¹H} NMR (243 MHz, [D₈]toluene, -55°C): δ = -6.4 (d, ²J(P,P) = 219.5 Hz; PMe₃), 8.0 ppm (d, ²J(P,P) = 219.5 Hz; PMe₃); ¹H-¹³C HSQC NMR (f1 = 600 MHz, f2 = 151 MHz, [D₈]toluene, -30°C, J = 145.0 Hz, ¹³C projection, selected resonances): δ = 85.2 (η²-O=C), 86.1 ppm (η²-O=C).

Complex 24: ¹H NMR (600 MHz, C₆D₆): δ = 1.07 (d, ³J(H,H) = 6.6 Hz, 6H; 2CH₃, NAr), 1.12 (m, 15H; 2CH₃, NAr and PMe₃), 3.43 (s, 1H; η²-O=CH), 3.43 (sept, ³J(H,H) = 6.6 Hz, 2H; 2CH, NAr), 5.86 (s, 1H; η²-O=CH), 6.80–6.88 (m, 5H; *o*-H and *p*-H, η²-O=CPh and *m*-H, NAr), 6.94 (t, ³J(H,H) = 8.4 Hz, 1H; *p*-H, NAr), 6.99 (t, ³J(H,H) = 7.2 Hz, 1H; *p*-H, η²-O=CPh), 7.08 (t, ³J(H,H) = 7.8 Hz, 2H; *m*-H, η²-O=CPh), 7.27 (t, ³J(H,H) = 7.2 Hz, 2H; *m*-H, η²-O=CPh), 7.50 ppm (d, ³J(H,H) = 7.8 Hz, 2H; *o*-H, η²-O=CPh); ³¹P{¹H} NMR (243 MHz, C₆D₆): δ = -1.0 ppm (s; PMe₃); ¹³C{¹H} NMR (151 MHz, C₆D₆): δ = 10.8 (d, ²J(C,P) = 22.6 Hz; PMe₃), 22.9 (s; 2CH₃, NAr), 24.2 (s; 2CH₃, NAr), 28.2 (s; 2CH, NAr), 75.1 (s; η²-O=C), 84.6 (s; η²-O=C), 122.4, 123.4, 125.1, 125.2, 125.3, 128.3, 128.4, 128.6, 143.4, 147.8, 147.9, 153.1 ppm (all of the aromatic carbon atoms of NAr and two η²-O=CPh ligands); IR (nujol): $\tilde{\nu}$ = 1596 (s; C=O), 1487 cm⁻¹ (s; C=O); elemental analysis calcd (%) for C₂₉H₃₈MoNO₂P (559.530): C 62.25, H 6.85, N 2.50; found: C 62.22, H 6.95, N 2.30.

Complex 25: ¹H NMR (600 MHz, [D₈]toluene, 0°C): δ = 0.77 (d, ²J(H,P) = 6.0 Hz, 9H; PMe₃), 1.08 (d, ²J(H,P) = 7.2 Hz, 9H; PMe₃), all of the CH₃ signals for the NAr ligand were within the range 1.12–1.21 (by ¹H-¹H COSY NMR) and were obscured by the aliphatic resonances of compounds 3 and 24 that were present in the mixture, 1.25 (br s, 9H; PMe₃), 3.71 (sept, ³J(H,H) = 7.2 Hz, 1H; CH, NAr), 3.90 (sept, ³J(H,H) = 6.6 Hz, 1H; CH, NAr), 5.59 ppm (t, ³J(H,P) = 4.8 Hz, 1H; η²-O=CH), all of the aromatic signals overlapped with the resonances of PhHSi(OBn)₂, complexes 3 and 24, and residual C₆D₆; ³¹P{¹H} NMR (243 MHz, [D₈]toluene, 0°C): δ = -10.4 (d, ²J(P,P) = 255.1 Hz, 1P; PMe₃), -0.21 (dd, ²J(P,P) = 9.7 Hz and 255.1 Hz, 1P; PMe₃), 8.5 ppm (vt, ²J(P,P) = 9.7 Hz, 1P; PMe₃); ¹H-¹³C HSQC NMR (f1 = 600 MHz, f2 = 151 MHz, [D₈]toluene, -30°C, J = 145.0 Hz, ¹³C projection, selected resonances): δ = 73.0 ppm (η²-O=C).

NMR-scale preparation of [(ArN=)Mo(SiH₂Ph)(OiPr)(PMe₃)₂] (18): Acetone (3.5 μL, 0.048 mmol) was added in one portion to a solution of complex 3 (29.2 mg, 0.048 mmol) in [D₈]toluene (0.6 mL) that was frozen in liquid N₂ in an NMR tube. The sample was immediately placed into a precooled NMR machine at -30°C. Upon increasing the temperature of the experiment, the reaction was monitored by NMR spectroscopy, which showed the very slow and selective transformation of complex 3 into complex 18 at 0°C. No intermediate compounds were observed below this temperature. Increasing the temperature of the experiment led to the faster formation of complex 18 and complete conversion was achieved after 1.3 h at RT. The 1D ¹H EXSY NMR spectra showed no exchange between free acetone and the OiPr group; however, RT 1D ³¹P EXSY NMR experiments revealed an intermolecular PMe₃ exchange. All of the volatile compounds were removed by evaporation to give brown oil, which was dried under vacuum and dissolved in C₆D₆. NMR analysis only showed the presence of complex 18 in solution. The product was fluxional at RT. The ¹H projection of the ¹H-¹³C HSQC NMR spectrum at -30°C showed a normal ¹J(H,C) = 138 Hz for the CH moiety in OiPr, thus ruling out the β-C-H agostic structure of complex 18. All attempts to isolate the product gave mixtures of complex 18 with unidentified decomposition products. ¹H NMR (600 MHz, [D₈]toluene, -28°C): δ = 1.11 (br s, 18H; 2PMe₃), 1.27 (d, ³J(H,H) = 5.5 Hz, 6H; 2CH₃, OiPr), 1.39 (d, ³J(H,H) = 6.6 Hz, 12H; 4CH₃, NAr), 3.84 (sept, ³J(H,H) = 6.6 Hz, 1H; CH, NAr), 4.12 (sept, ³J(H,H) = 6.6 Hz, 1H; CH, NAr), 4.24 (br s, 1H; CH, OiPr), 5.82 (br s, 2H; SiH₂), 6.94–7.24 (m, 3H; *m*-H and *p*-H, NAr, the peaks overlapped with signals of residual [D₈]toluene), 7.25 (t, ³J(H,H) = 6.9 Hz, 1H; *p*-H, SiPh), 7.34 (t, ³J(H,H) = 6.9 Hz, 2H; *m*-H, SiPh), 8.04 ppm (d, ³J(H,H) = 6.9 Hz, 2H; *o*-H, SiPh); ³¹P{¹H} NMR (243 MHz, [D₈]toluene, 22°C): δ = -5.9 ppm (s; 2PMe₃); ¹³C{¹H} NMR (151 MHz, [D₈]toluene, 0°C): δ = 152.7, 148.3, 136.5 (s; *o*-C, SiPh), 126.91, 126.87, 126.6, 123.5, 123.1 (all of the aromatic carbon atoms of NAr and SiPh), 72.4 (s; OCH), 30.1 (br s; CH, NAr), 27.2 (br s; CH, NAr), 25.0 (s; CH₃, OiPr), 24.9 (s; CH₃, OiPr), 24.6 (br s; CH₃, NAr), 23.7 (br s; CH₃, NAr), 16.1 ppm (d, ¹J(C,P) = 13.6 Hz; PMe₃); ¹H-²⁹Si HSQC NMR (f1 = 300 MHz, f2 = 59.6 MHz, J = 200 Hz, C₆D₆, ²⁹Si projection): δ = 4.9 ppm (SiH₂Ph).

NMR-scale reaction of complex 18 with PMe₃: PMe₃ (46.8 μL, 0.615 mmol) was added in one portion to a solution of complex 16 (which was generated in situ from complex 3 (24.9 mg, 0.041 mmol) and

acetone (3.0 μL , 0.041 mmol); PMe_3 that was released during the reaction was removed under vacuum) in C_6D_6 (0.6 mL) at RT in an NMR tube. The reaction mixture was left to stand at RT for 5 min. NMR analysis showed the complete conversion of complex **18** and the formation of complex **3** with the release of one equivalent of acetone.

NMR-scale reaction of complex 18 with acetone: Acetone (40.4 μL , 0.55 mmol) was added to a solution of complex **18** (which was generated in situ from complex **3** (16.7 mg, 0.028 mmol) and acetone (2.0 μL , 0.028 mmol)) in C_6D_6 (0.6 mL) in an NMR tube. The reaction was monitored by NMR spectroscopy overnight at RT, which showed the slow (12 h) conversion of complex **18** into $[(\text{ArN}=\text{Mo}(\text{SiH}_2\text{Ph})(\kappa^2\text{-O-C}(\text{Me})_2\text{CH}_2\text{C}(\text{O})\text{Me})(\text{PMe}_3))] (\mathbf{20})$, accompanied by the release of one equivalent of PMe_3 . ^1H NMR (300 MHz, C_6D_6): $\delta = 1.01$ (d, $^2J(\text{H},\text{P}) = 9.0$ Hz, 9H; PMe_3), 1.26 (d, $^3J(\text{H},\text{H}) = 6.6$ Hz, 6H; 2CH_3 , NAr), 1.32 (m, 9H; 2CH_3 , NAr and CH_3 , $\eta^2\text{-OC}(\text{Me})_2\text{CH}_2\text{C}(\text{O})\text{Me}$), 1.42 (m, 3H; CH_3 , $\eta^2\text{-OC}(\text{Me})_2\text{CH}_2\text{C}(\text{O})\text{Me}$), 2.16 (d, $^2J(\text{H},\text{H}) = 12.9$ Hz, 1H; $\eta^2\text{-OC}(\text{Me})_2\text{CH}_2\text{C}(\text{O})\text{Me}$), 2.23 (s, 3H; $\eta^2\text{-OC}(\text{Me})_2\text{CH}_2\text{C}(\text{O})\text{Me}$), 2.59 (d, $^2J(\text{H},\text{H}) = 12.9$ Hz, 1H; $\eta^2\text{-OC}(\text{Me})_2\text{CH}_2\text{C}(\text{O})\text{Me}$), 4.01 (sept, $^3J(\text{H},\text{H}) = 6.9$ Hz, 1H; CH, NAr), 4.07 (sept, $^3J(\text{H},\text{H}) = 6.6$ Hz, 1H; CH, NAr), 5.87 (m, 2H; SiH_2), 6.98 (m, 3H; *m*-H and *p*-H, NAr), 7.23 (m, 3H; *m*-H and *p*-H, SiPh), 7.80 ppm (m, 2H; *o*-H, SiPh); $^{31}\text{P}\{^1\text{H}\}$ NMR (121.5 MHz, C_6D_6): $\delta = -6.7$ ppm (s; PMe_3).

NMR-scale reaction of complex 18 with PhSiH_3 : *Method A: Room-temperature reaction in the presence of PMe_3 :* PhSiH_3 (5.0 μL , 0.041 mmol) and PMe_3 (4.2 μL , 0.041 mmol) were simultaneously added in one portion to a solution of complex **18** (which was generated in situ from complex **3** (24.9 mg, 0.041 mmol) and acetone (3.0 μL , 0.041 mmol)) in C_6D_6 (0.6 mL) at RT in an NMR tube. The reaction mixture was left to stand at RT for 5 min. NMR analysis showed the complete conversion of complex **18** and the selective regeneration of complex **3**, accompanied by the release of $\text{PhH}_2\text{Si}(\text{O}i\text{Pr})$.

Method B: Low-temperature VT reaction: PhSiH_3 (7.6 μL , 0.062 mmol) was added in one portion to a solution of complex **18** (which was prepared in situ from complex **3** (37.6 mg, 0.062 mmol) and acetone (22.7 μL , 0.309 mmol); excess acetone and PMe_3 that was released during the reaction were removed under vacuum) in $[\text{D}_8]\text{toluene}$ (0.6 mL) that was frozen in liquid N_2 in an NMR tube. The mixture was immediately placed into a pre-cooled NMR machine at -30°C and the temperature was lowered to -50°C . Then, the temperature of the experiment was gradually increased and the reaction was monitored by NMR spectroscopy, which showed the release of $\text{PhH}_2\text{Si}(\text{O}i\text{Pr})$ and $\text{PhHSi}(\text{O}i\text{Pr})_2$ at -45°C and the formation of $[(\text{ArN}=\text{Mo}(\text{H})_2(\text{SiH}_2\text{Ph})_2(\text{PMe}_3)_2)] (\mathbf{19})$, as a mixture of two isomers in the ratio 10:1, according to $^{31}\text{P}\{^1\text{H}\}$ NMR spectroscopy. Increasing the temperature of the experiment did not allow us to observe any other intermediates. The sole formation of complex **3** was observed upon warming the sample to RT.

Complex 19: ^1H NMR (600 MHz, $[\text{D}_8]\text{toluene}$, -45°C , major isomer): $\delta = 0.77$ (br s, 9H; PMe_3), 0.93 (br s, 6H; 2CH_3 , NAr), 1.04 (br s, 6H; 2CH_3 , NAr), 1.13 (br s, 6H; 2CH_3 , NAr), 1.17 (br s, 9H; PMe_3), 1.23 (br s, 6H; 2CH_3 , NAr), 2.53 (t, $^2J(\text{H},\text{P}) = 42.0$ Hz, 1H; MoH), 3.50 (d, $^2J(\text{H},\text{P}) = 25.7$ Hz, 1H; MoH), 4.10 (br s, 2H; 2CH , NAr), 5.06 (d, $^3J(\text{H},\text{P}) = 21.8$ Hz, 1H; SiH_2), 5.51 (br s, 1H; SiH_2), 5.78 (br d, $^2J(\text{H},\text{P}) = 15.8$ Hz, 1H; SiH_2), 6.04 (br s, 1H; SiH_2), 6.73 (br s, 2H; overlapping signals of *p*-H, 2SiPh), 6.86–7.40 (5H; *m*-H, NAr and SiPh, *p*-H, NAr, the signals overlapped with resonances of residual $[\text{D}_8]\text{toluene}$), 7.41 (br s, 2H; *m*-H, SiPh), 7.96 (br s, 2H; *o*-H, SiPh), 8.45 ppm (br s, 2H; *o*-H, SiPh); $^1\text{H}\{^{31}\text{P}\}$ NMR (600 MHz, $[\text{D}_8]\text{toluene}$, -45°C , major isomer, selected resonances): $\delta = 2.53$ (br s, 1H; MoH), 3.50 (br s, 1H; MoH), 5.05 (br s, 1H; SiH_2), 5.51 (br s, 1H; SiH_2), 5.78 (br s, 1H; SiH_2), 6.04 ppm (br s, 1H; SiH_2); ^1H NMR (selectively decoupled from one PMe_3 group at $\delta = -32.9$ ppm in the $^{31}\text{P}\{^1\text{H}\}$ NMR spectrum), 600 MHz, $[\text{D}_8]\text{toluene}$, -45°C , major isomer, selected resonances): $\delta = 2.51$ (br d, $^2J(\text{H},\text{P}) = 41.0$ Hz, 1H; MoH), 3.53 (d, $^2J(\text{H},\text{P}) = 25.7$ Hz, 1H; MoH), 5.03 (d, $^2J(\text{H},\text{P}) = 21.8$ Hz, 1H; SiH_2), 5.50 (br s, 1H; SiH_2), 5.79 (br t, $^3J(\text{H},\text{P}) = 7.0$ Hz, 1H; SiH_2), 5.99 ppm (br s, 1H; SiH_2); ^1H NMR (selectively decoupled from one PMe_3 group at -12.5 ppm in the $^{31}\text{P}\{^1\text{H}\}$ NMR spectrum), 600 MHz, $[\text{D}_8]\text{toluene}$, -45°C , major isomer, selected resonances): $\delta = 2.51$ (br d, $^2J(\text{H},\text{P}) = 41.6$ Hz, 1H; MoH), 3.52 (br s, 1H; MoH), 5.03

(br s, 1H; SiH_2), 5.50 (d, $^3J(\text{H},\text{P}) = 10.6$ Hz, 1H; SiH_2), 5.8 (br t, $^3J(\text{H},\text{P}) = 6.9$ Hz, 1H; SiH_2), 5.99 ppm (br s, 1H; SiH_2); $^{31}\text{P}\{^1\text{H}\}$ NMR (243 MHz, $[\text{D}_8]\text{toluene}$, -45°C): $\delta = -37.6$ (d, $^2J(\text{P},\text{P}) = 32.1$ Hz, PMe_3 , minor isomer), -32.9 (d, $^2J(\text{P},\text{P}) = 32.7$ Hz, PMe_3 , major isomer), -12.5 (d, $^2J(\text{P},\text{P}) = 32.7$ Hz, PMe_3 , major isomer), -6.4 ppm (d, $^2J(\text{P},\text{P}) = 32.1$ Hz, PMe_3 , minor isomer). ^{31}P NMR (selectively decoupled from Me groups at $\delta = 1.17$ ppm in the ^1H NMR spectrum, 243 MHz, $[\text{D}_8]\text{toluene}$, -30°C , major isomer): $\delta = -12.8$ (t, $J(\text{P},\text{H}) = 34.9$ Hz; PMe_3), -33.4 ppm (br s; PMe_3); ^{31}P NMR (selectively decoupled from Me groups at $\delta = 0.77$ ppm in the ^1H NMR spectrum, 243 MHz, $[\text{D}_8]\text{toluene}$, -30°C , major isomer): $\delta = -12.8$ (br s; PMe_3), -33.3 ppm (br s; PMe_3); $^{13}\text{C}\{^1\text{H}\}$ NMR (151 MHz, $[\text{D}_8]\text{toluene}$, -50°C , major isomer): $\delta = 17.0$ (d, $^1J(\text{C},\text{P}) = 21.1$ Hz; PMe_3), 19.6 (d, $^1J(\text{C},\text{P}) = 26.7$ Hz; PMe_3), 23.3 (s; CH_3 , NAr), 24.5 (s; CH_3 , NAr), 25.0 (s; CH_3 , NAr), 25.6 (s; CH_3 , NAr), 27.1 (s; CH, NAr), 122.9 (s; *p*-H, SiPh), 135.8 (s; *m*-C, SiPh), 136.0 (s; *o*-C, SiPh), 137.6 ppm (s; *o*-C, SiPh). ^{29}Si INEPT+ NMR (119.2 MHz, $[\text{D}_8]\text{toluene}$, -50°C , $J = 200$ Hz, major isomer): $\delta = -12.1$ ppm (two doublets, $^1J(\text{Si},\text{H}) = 160.4$ Hz and 171.7 Hz; overlapping resonances for two SiH_2Ph groups).

NMR-scale reaction of complex 18 with (*m*-Tol) SiH_3 : (*m*-Tol) SiH_3 (3.5 μL , 0.028 mmol) and PMe_3 (2.8 μL , 0.028 mmol) were added simultaneously in one portion to a solution of complex **18** (which was generated in situ from complex **3** (16.7 mg, 0.028 mmol) and acetone (2.0 μL , 0.028 mmol)) in C_6D_6 (0.6 mL) at RT in an NMR tube. The reaction mixture was left for 15 min at RT. NMR analysis showed the formation of complex **3** and (*m*-Tol) $\text{H}_2\text{Si}(\text{O}i\text{Pr})$. The formation of (*m*-Tol) $\text{H}_2\text{Si}(\text{O}i\text{Pr})$ was suggested on the basis of a series of ^1H – ^{13}C and ^1H – ^1H 2D NMR experiments; however, busy NMR spectra prevented the characterization of the hydrosilylation product. Exclusive formation of complex **3** was also observed in the NMR-scale reactions of complex **18** with PhMeSiH_2 and PhMe_2SiH , which were performed in an analogous manner to the reaction of complex **18** with PhSiH_3 .

NMR-scale reaction of complex 18 with benzaldehyde: Benzaldehyde (19.5 μL , 0.193 mmol) was added in one portion to a solution of complex **18** (which was generated in situ from complex **3** (29.2 mg, 0.048 mmol) and acetone (3.5 μL , 0.048 mmol)) in C_6D_6 (0.6 mL) at RT in an NMR tube. The color of the mixture changed to a different tint of brown almost immediately. NMR analysis after 10 min at RT showed the release of acetone and the selective formation of bis(benzaldehyde) complex **23** and $\text{PhHSi}(\text{O}i\text{Pr})_2$.

NMR-scale reaction of complex 18 with cyclohexanone: Cyclohexanone (20.0 μL , 0.193 mmol) was added in one portion at RT to a solution of complex **18** (which was generated in situ from complex **3** (23.4 mg, 0.039 mmol) and acetone (14.1 μL , 0.193 mmol); excess $\text{Me}_2\text{C}(\text{O})$ and PMe_3 that was released during the reaction were removed under vacuum) in C_6D_6 (0.6 mL) in an NMR tube. The reaction mixture was left to stand at RT, overnight. NMR analysis showed the formation of a mixture of complex **18** and $[(\text{ArN}=\text{Mo}(\text{SiH}_2\text{Ph})(\text{OCy})(\text{PMe}_3)_2)] (\mathbf{22})$; 1:1, according to the $^{31}\text{P}\{^1\text{H}\}$ NMR spectrum) and the release of acetone.

Preparation of $[(\text{ArN}=\text{Mo}(\text{SiH}_2\text{Ph})(\text{OCy})(\text{PMe}_3)_2)] (\mathbf{22})$: Cyclohexanone (7.0 μL , 0.067 mmol) was added in one portion to a solution of complex **3** (37.1 mg, 0.061 mmol) in C_6D_6 (0.6 mL) at RT in an NMR tube. The reaction mixture was left to stand at RT for 30 min. NMR analysis showed the complete conversion of the starting material, the release of one equivalent of PMe_3 , and the selective formation of complex **22**. All of the volatile compounds were removed by evaporation. The residue was dried under vacuum and extracted with Et_2O (4 mL). The solution was concentrated to about 2 mL and left to stand at -30°C for 2 days, thereby affording the precipitation of brown crystals, which were filtered off and dried under vacuum. Yield: 11.1 mg, 29%. The product was fluxional at RT. ^1H NMR (300 MHz, C_6D_6): $\delta = 7.99$ (br d, $^3J(\text{H},\text{H}) = 6.9$ Hz, 2H; *o*-H, SiPh), 7.00–7.30 (m, 6H; *m*-H and *p*-H, NAr and SiPh), 5.75 (br s, 2H; SiH_2), 4.06 (br s, 1H; CH, NAr), 3.98 (br s, 1H; CH, NAr), 3.88 (br s, 1H; OCH), 0.81–1.92 (m, 22H; 4CH_3 , NAr and 5CH_2 , OCy), 1.13 ppm (br s, 18H; 2PMe_3 , as determined by ^1H – ^{31}P HSQC NMR); $^{31}\text{P}\{^1\text{H}\}$ NMR (121.5 MHz, C_6D_6): $\delta = -5.8$ ppm (s; 2PMe_3).

NMR-scale reaction of complex 18 with benzonitrile: PhCN (3.2 μL , 0.028 mmol) was added in one portion at RT to a solution of complex **18** (which was generated in situ from complex **3** (16.7 mg, 0.028 mmol) and

acetone (2.0 μ L, 0.028 mmol)) in C_6D_6 (0.6 mL) in an NMR tube. No visual change was observed after the addition of PhCN and the reaction mixture was left to stand at RT for 2 h. Subsequent NMR analysis showed the complete conversion of complex **18** and the formation of $[(ArN=)Mo(SiH_2Ph)(N=CHPh)(\eta^2-Me_2C(O))(PMe_3)_2]$ (**21**; 70% yield, by $^{31}P\{^1H\}$ NMR spectroscopy; approximate 1:1 mixture of the *cis* and *trans* isomers). 1H NMR (300 MHz, C_6D_6 , mixture of isomers): δ = 1.09 (m; 2 PMe_3 for each isomer, both isomers), 1.32 (d, $^3J(H,H)$ = 6.9 Hz, 6H; 2 CH_3 , NAr, both isomers), 1.38 (d, $^3J(H,H)$ = 6.9 Hz, 6H; 2 CH_3 , NAr, both isomers), 1.59 (m; 4 CH_3 , $\eta^2-Me_2C(O)$, both isomers), 4.18 (sept, $^3J(H,H)$ = 6.9 Hz, 1H; CH, NAr, one isomer), 4.36 (sept, $^3J(H,H)$ = 6.9 Hz, 1H; CH, NAr, one isomer), 5.50 (t, $^3J(H,P)$ = 5.7 Hz, 2H; SiH_2 , one isomer), 5.61 (t, $^3J(H,P)$ = 6.0 Hz, 2H; SiH_2 , one isomer), 6.80–7.55 (m; overlapping aromatic protons for both isomers), 7.83 (m, 2H; *o*-H, CPh, one isomer), 7.96 (m, 1H; N=CH, one isomer), 8.38 ppm (m, 2H; *o*-C, Ph, one isomer); $^{31}P\{^1H\}$ NMR (121.5 MHz, C_6D_6 , mixture of isomers): δ = 2.3 (s; 2 PMe_3 , one isomer), 2.8 ppm (s; 2 PMe_3 , one isomer). **NMR-scale reaction of complex 3 with PhCN:** PhCN (6.4 μ L, 0.055 mmol) was added in one portion to a solution of complex **3** (16.8 mg, 0.028 mmol) in C_6D_6 (0.6 mL) at RT in an NMR tube. The reaction mixture was left to stand for 1 h at RT. NMR analysis showed the selective formation of $[(ArN=)Mo(SiH_2Ph)(N=CHPh)(NCPH)(PMe_3)_2]$ (**34**, approximate 1:1 mixture of isomers), accompanied by the release of one equivalent of PMe_3 . The reaction mixture was monitored by NMR spectroscopy for an additional 36 h at RT, which showed the selective rearrangement of complex **34** into $[(ArN=)Mo(SiH_2Ph)(\kappa^3-N=C(Ph)-N=CHPh)(PMe_3)]$ (**35**), accompanied by the release of another equivalent of PMe_3 .

Complex 34: 1H NMR (300 MHz, C_6D_6 , both isomers): δ = 1.22 (m; 2 PMe_3 for each isomer, overlapping signals of both isomers, total 36H), 1.44 (d, $^3J(H,H)$ = 6.9 Hz; 2 CH_3 , NAr for each isomer, total 12H), 1.50 (d, $^3J(H,H)$ = 6.9 Hz; 2 CH_3 , NAr for each isomer, total 12H), 4.30 (sept, $^3J(H,H)$ = 6.9 Hz, 2H; 2CH, NAr of one isomer), 4.48 (sept, $^3J(H,H)$ = 6.9 Hz, 2H; 2CH, NAr of one isomer), 5.62 (t, $^3J(H,P)$ = 5.7 Hz, 2H; SiH_2 of one isomer), 5.73 (t, $^3J(H,P)$ = 6.3 Hz, 2H; SiH_2 of one isomer), 6.92–7.54 (m; overlapping aromatic signals of NAr, SiPh, and 2CPh for both isomers), 7.68 (d, $^3J(H,H)$ = 7.5 Hz, 2H; *o*-H, CPh, one isomer), 7.93 (t, $J(H,P)$ = 6.6 Hz, 1H; N=CH, one isomer), 7.96 (d, $^3J(H,H)$ = 7.5 Hz, 2H; *o*-H, CPh, one isomer), 8.08 (d, $^3J(H,H)$ = 7.5 Hz, 2H; *o*-H, CPh, one isomer), 8.50 ppm (t, $J(H,P)$ = 7.2 Hz, 1H; N=CHPh, one isomer); $^{31}P\{^1H\}$ NMR (121.5 MHz, C_6D_6 , both isomers): δ = 2.8 (s; 2 PMe_3 , one isomer), 2.3 ppm (s; 2 PMe_3 , another isomer). ^{29}Si INEPT+ NMR (119.2 MHz, C_6D_6 , J = 200 Hz, both isomers): δ = -12.6 (t, $^1J(Si,H)$ = 151.4 Hz; SiH_2Ph , one isomer), -19.9 ppm (t, $^1J(Si,H)$ = 149.1 Hz; SiH_2Ph , one isomer); $^{13}C\{^1H\}$ NMR (151 MHz, C_6D_6 , both isomers, selected resonances): δ = 197.1 (s; N=CH, one isomer), 153.0 (s; N=CH, one isomer), 136.4 (s; *o*-C, CPh, one isomer), 134.9 (s; *o*-C, CPh, one isomer), 28.1 (s; CH, NAr, one isomer), 28.0 (s; CH, NAr, one isomer), 23.9 (s; CH_3 , NAr, one isomer), 23.6 (s; CH_3 , NAr, one isomer), 16.6 (vt, $^1J(C,P)$ = 24.2 Hz; PMe_3 , one isomer), 15.1 ppm (vt, $^1J(C,P)$ = 24.2 Hz; PMe_3 , one isomer).

Complex 35: 1H NMR (300 MHz, C_6D_6): δ = 1.17 (d, $^3J(H,H)$ = 6.6 Hz, 6H; 2 CH_3 , NAr), 1.21 (d, $^3J(H,H)$ = 6.6 Hz, 6H; 2 CH_3 , NAr), 1.57 (d, $^2J(H,P)$ = 9.0 Hz, 9H; PMe_3), 3.58 (sept, $^3J(H,H)$ = 6.6 Hz, 2H; 2CH, NAr), 5.28 (s, 1H; $\eta^3-N=C(Ph)-N=CHPh$), 5.84 (d, $^2J(H,H)$ = 10.8 Hz, 1H; SiH_2), 5.96 (d, $^2J(H,H)$ = 10.8 Hz, 1H; SiH_2), 6.64–7.32 (m, 14H; *m*-H and *p*-H, NAr and 2CPh, *m*-H, *p*-H, and *o*-H, SiPh), 7.86 (m, 2H; *o*-H, CPh), 8.11 ppm (m, 2H; *o*-H, CPh); $^{31}P\{^1H\}$ NMR (121.5 MHz, C_6D_6): δ = 4.8 ppm (s; PMe_3); $^{13}C\{^1H\}$ NMR (75.5 MHz, C_6D_6): δ = 197.1 (s; $\eta^3-N=C(Ph)-N=CHPh$), 153.0 (s; *i*-C), 150.3 (s; *i*-C), 144.7 (s), 135.8 (s; *i*-C), 134.9 (s; *o*-C, CPh), 132.7 (s; *o*-C, CPh), 131.7 (s; *o*-C, CPh), 127.7, 123.9, 122.4 (aromatic carbon atoms overlap with the signal of C_6D_6), 54.7 (s, $\eta^3-N=C(Ph)-N=CHPh$), 28.2 (s; CH, NAr), 23.3 (s; CH_3 , NAr), 23.2 (s; CH_3 , NAr), 14.1 ppm (d, $^1J(C,P)$ = 24.1 Hz; PMe_3); ^{29}Si INEPT+ NMR (119.2 MHz, C_6D_6 ; J = 200 Hz): δ = -25.4 ppm (td, $^1J(Si,H)$ = 203.9 Hz, $^2J(Si,P)$ = 6.0 Hz; SiH_2Ph).

General procedure for the hydrosilylation reactions: A solution of the organic substrate (0.06 M) and silane (1:1 ratio) and TMS (5 mol%) in C_6D_6

(0.6 mL) was added to complex **3** (5 mol%) in one portion at RT. The mixture was immediately transferred into an NMR tube. Depending on the substrate, the reaction was monitored by NMR spectroscopy, either at RT or at 50°C. The structures of all of the products were determined by NMR analysis. The conversions of the organic substrates and the yields of the products were calculated by NMR spectroscopy with TMS as an internal standard.

X-ray structure analysis: Crystals of compounds **3** and **24** were grown from solutions in Et₂O by cooling to -30°C. The crystals were mounted in a film of perfluoropolyether oil onto a glass fiber and transferred onto a Bruker three-circle diffractometer with a CCD detector (SMART system). The data were corrected for Lorentz and polarization effects. The structures were solved by using direct methods and were refined by full-matrix least-squares procedures.^[58] All non-hydrogen atoms were refined anisotropically. In the case of complex **3**, all hydrogen atoms were located from Fourier difference synthesis and refined isotropically. In the case of complex **24**, hydrogen atoms were placed at calculated positions and refined with the “riding” model. The location and magnitude of the residual electron density was of no chemical significance. Crystal data for complex **3** have been reported in a previous communication.^[19] CCDC-818200 (**3**) and CCDC-936407 (**24**) contain the supplementary crystallographic data for this paper. These data can be obtained free of charge from TheCambridge Crystallographic Data Centre via www.ccdc.cam.ac.uk/data_request/cif.

Crystal data for complex 24: Brown/yellow blocks; $C_{29}H_{38}MoNO_2P$; M_w = 559.51; crystal size: 0.34 × 0.26 × 0.22 mm³; monoclinic; space group $P2_1/n$; a = 10.9983(4), b = 18.5204(6), c = 13.6935(4) Å; α = 90, β = 93.261(2), γ = 90°; V = 2784.75(16) Å³; Z = 4; ρ_{calcd} = 1.335 g cm⁻³; T = 123(2) K; μ = 0.553 mm⁻¹; λ = 0.71070 Å; $2\theta_{max}$ = 59.4°; 24780 measured reflections; 8084 unique reflections; 307 parameters; $R1$ = 0.0440, $wR2$ = 0.1007 (5632 observed reflections with $I \geq 2\sigma(I)$); $R1$ = 0.0752, $wR2$ = 0.1110 (all data); GOF = 0.949; largest peak in the final difference Fourier map had an electron density of 1.324 e Å⁻³ and the lowest hole was of -1.324 e Å⁻³.

DFT calculations: The unconstrained geometry optimization was performed for all of the considered structures with the Gaussian03 program package^[59] by using DFT and by applying the Becke three-parameter hybrid-exchange functional in conjunction with the gradient-corrected nonlocal correlation functional of Perdew and Wang (B3PW91).^[60] The 6-31G(d,p) basis set was used for the H, C, N, O, Si, P, and Cl atoms. The Hay–Wadt effective core potentials (ECPs) and the corresponding VDZ basis sets were used for the Mo atoms.^[61] The same level of theory was used in the frequency calculations that were performed at the located stationary points. The thermodynamic parameters were calculated in the rigid rotor-harmonic oscillator approximation.

Acknowledgements

This work was supported by the Petroleum Research Fund of the American Chemical Society (grant to G.I.N.) and by an OGS fellowship to A.Y.K. S.K.I. thanks the Russian Foundation for Basic Research and L.G.K. and J.A.K.H. thank the Royal Society (London) for support. We also thank the University of Durham for the use of their X-ray facilities.

- [1] a) M. Hudlicky, *Reductions in Organic Chemistry*, ACS monograph, 188, **1996**; b) R. C. Larock, *Comprehensive Organic Transformations: A Guide to Functional Group Preparation*, 2nd ed., Wiley-VCH, Weinheim, **1999**; c) *The Chemistry of Functional Groups* (Ed: S. Patai), Wiley, New York, **1966**; d) *Comprehensive Organic Chemistry*, Vol. 3, (Eds: D. Barton, W. D. Ollis), Pergamon, Oxford, **1979**.
[2] a) *Hydrosilylation, Advances in Silicon Science* (Ed.: B. Marciniec), Springer, Heidelberg, **2009**; b) A. K. Roy, *Adv. Organomet. Chem.* **2007**, 55, 1; c) S. E. Gibson, M. Rudd, *Adv. Synth. Catal.* **2007**, 349, 781; d) B. Marciniec, *Appl. Organomet. Chem.* **2000**, 14, 527; e) R. Noyori, *Asymmetric Catalysis in Organic Synthesis*, Wiley, New

- York, **1994**; f) I. Ojima, *Catalytic Asymmetric Synthesis*, VCH, Weinheim, **1993**; g) H. Brunner, W. Zettmeier, *Handbook of Enantioselective Catalysis with Transition Metal Compounds*, VCH, Weinheim, **1993**; h) I. Ojima, in *The Chemistry of Organic Silicon Compounds* (Eds.: S. Patai, Z. Rappoport), Wiley, New York, **1989**.
- [3] For reviews on Fe catalysis, see: a) K. Junge, K. Schröder, M. Beller, *Chem. Commun.* **2011**, 47, 4849; b) D. Addis, S. Das, K. Junge, M. Beller, *Angew. Chem.* **2011**, 123, 6128; *Angew. Chem. Int. Ed.* **2011**, 50, 6004; c) S. Chakraborty, H. Guan, *Dalton Trans.* **2010**, 39, 7427; d) M. Zhang, A. Zhang, *Appl. Organomet. Chem.* **2010**, 24, 751; e) S. Díez-González, S. Nolan, *Org. Prep. Proced.* **2007**, 39, 523.
- [4] For Ti and Zr catalysis, see: a) S. C. Berk, K. A. Kreuzer, S. L. Buchwald, *J. Am. Chem. Soc.* **1991**, 113, 5093; b) S. C. Berk, S. L. Buchwald, *J. Org. Chem.* **1992**, 57, 3751; c) R. D. Broene, S. L. Buchwald, *J. Am. Chem. Soc.* **1993**, 115, 12569; d) M. B. Carter, B. Schjøtt, A. Gutiérrez, S. L. Buchwald, *J. Am. Chem. Soc.* **1994**, 116, 11667; e) R. L. Halterman, T. M. Ramsey, Z. J. Chen, *Org. Chem.* **1994**, 59, 2642; f) J. F. Harrod, S. Xin, *Can. J. Chem.* **1995**, 73, 999; g) S. S. Yun, S. Y. Yong, S. Lee, *Bull. Korean Chem. Soc.* **1997**, 18, 1058; h) J. Yun, S. L. Buchwald, *J. Am. Chem. Soc.* **1999**, 121, 5640.
- [5] For Mn catalysis, see: a) S. U. Son, S.-J. Paik, I. S. Lee, Y. A. Lee, Y. K. Chung, W. K. Seok, H. N. Lee, *Organometallics* **1999**, 18, 4114; b) S. U. Son, S.-J. Paik, Y. K. Chung, *J. Mol. Catal. A* **2000**, 151, 87.
- [6] For Co catalysis, see: F. Yu, X.-C. Zhang, F.-F. Wu, J.-N. Zhou, W. Fang, J. Wu, A. S. C. Chan, *Org. Biomol. Chem.* **2011**, 9, 5652.
- [7] For Ni catalysis, see: a) F.-G. Fontaine, R.-V. Nguyen, D. Zargarian, *Can. J. Chem.* **2003**, 81, 1299; b) S. Chakraborty, J. A. Krause, H. Guan, *Organometallics* **2009**, 28, 582; c) B. L. Tran, M. Pink, D. J. Mendiola, *Organometallics* **2009**, 28, 2234.
- [8] For Cu catalysis, see reviews: a) C. Deutsch, N. Krause, B. H. Lipshutz, *Chem. Rev.* **2008**, 108, 2916; b) S. Díez-González, S. P. Nolan, *Acc. Chem. Res.* **2008**, 41, 349.
- [9] For Re catalysis, see: a) G. D. Du, P. E. Fanwick, M. M. Abu-Omar, *J. Am. Chem. Soc.* **2007**, 129, 5180; b) K. A. Nolin, J. R. Krumper, M. D. Pluth, R. G. Bergman, F. D. Toste, *J. Am. Chem. Soc.* **2007**, 129, 14684; c) E. A. Ison, E. R. Trivedi, R. A. Corbin, M. M. Abu-Omar, *J. Am. Chem. Soc.* **2005**, 127, 15374; d) G. Du, M. M. Abu-Omar, *Organometallics* **2006**, 25, 4920; e) E. A. Ison, J. E. Cessarich, G. Du, P. E. Fanwick, M. M. Abu-Omar, *Inorg. Chem.* **2005**, 44, 2385; f) G. Du, P. E. Fanwick, M. M. Abu-Omar, *Inorg. Chim. Acta* **2008**, 361, 3184; g) B. Royo, C. C. Romão, *J. Mol. Catal. A* **2005**, 236, 107; h) K. A. Nolin, R. W. Ahn, Y. Kobayashi, J. J. Kennedy-Smith, F. D. Toste, *Chem. Eur. J.* **2010**, 16, 9555; i) P. M. Reis, B. Royo, *Catal. Commun.* **2007**, 8, 1057; j) R. G. de Noronha, C. C. Romão, A. C. Fernandes, *Tetrahedron Lett.* **2010**, 51, 1048; k) S. C. A. Sousa, A. C. Fernandes, *Adv. Synth. Catal.* **2010**, 352, 2218; l) J. L. Smeltz, P. D. Boyle, E. A. Ison, *Organometallics* **2012**, 31, 5994.
- [10] For Mo catalysts, see: a) J. C. C. Romão, E. Ziegler, G. Du, P. E. Fanwick, M. M. Abu-Omar, *Inorg. Chem.* **2009**, 48, 11290; c) M. Drees, T. Strassner, *Inorg. Chem.* **2007**, 46, 10850; d) P. J. Costa, C. C. Romão, A. C. Fernandes, B. Royo, P. Reis, M. J. Calhorda, *Chem. Eur. J.* **2007**, 13, 3934; e) P. M. Reis, C. C. Romão, B. Royo, *Dalton Trans.* **2006**, 1842; f) A. C. Fernandes, R. Fernandes, C. C. Romão, B. Royo, *Chem. Commun.* **2005**, 213; g) A. C. Fernandes, C. C. Romão, *Tetrahedron Lett.* **2005**, 46, 8881; h) C. A. Smith, L. E. Cross, K. Hughes, R. E. Davis, D. B. Judd, A. T. Merritt, *Tetrahedron Lett.* **2009**, 50, 4906.
- [11] For Mo catalysts developed by our group, see: a) A. Y. Khalimon, R. Simionescu, L. G. Kuzmina, J. A. K. Howard, G. I. Nikonov, *Angew. Chem.* **2008**, 120, 7815; *Angew. Chem. Int. Ed.* **2008**, 47, 7701; b) E. Peterson, A. Y. Khalimon, R. Simionescu, L. G. Kuzmina, J. A. K. Howard, G. I. Nikonov, *J. Am. Chem. Soc.* **2009**, 131, 908; c) O. G. Shirobokov, R. Simionescu, L. G. Kuzmina, G. I. Nikonov, *Chem. Commun.* **2010**, 46, 7831; d) O. G. Shirobokov, L. G. Kuzmina, G. I. Nikonov, *J. Am. Chem. Soc.* **2011**, 133, 6487; e) A. Y. Khalimon, R. Simionescu, G. I. Nikonov, *J. Am. Chem. Soc.* **2011**, 133, 7033; f) A. Y. Khalimon, O. G. Shirobokov, E. Peterson, R. Simionescu, L. G. Kuzmina, J. A. K. Howard, G. I. Nikonov, *Inorg. Chem.* **2012**, 51, 4300.
- [12] For example, see: O. Einsle, F. A. Texcan, S. L. A. Andrade, B. Schmid, M. Yoshida, J. B. Howard, D. C. Rees, *Science* **2002**, 297, 1696.
- [13] For examples of labile phosphine complexes of Mo, see refs. [11b,f]. For examples of inert phosphine complexes of Mo, see refs. [11c,d].
- [14] In the Ojima mechanism, a silyl hydride intermediate is formed upon the oxidative addition of the H–Si bond to the metal. The cycle is completed by the coordination of a carbonyl group to this species, the migration of the silicon atom onto the oxygen end of the carbonyl group to give an alkyl hydride intermediate, and the reductive elimination of the C–H bond: a) I. Ojima, in *The Chemistry of Organic Silicon Compounds* (Eds.: S. Patai, Z. Rappoport), Wiley, New York, **1989**; b) I. Ojima, T. Kogure, M. Kumagai, S. Horuchi, T. Sato, *J. Organomet. Chem.* **1976**, 122, 83; c) J. F. Peyronel, H. B. Kagan, *Nouv. J. Chim.* **1978**, 2, 211.
- [15] a) N. Kaltsoyannis, P. Mountford, *J. Chem. Soc. Dalton Trans.* **1999**, 781; b) W. A. Nugent, J. M. Mayer, *Metal–Ligand Multiple Bonds*, Wiley, New York, **1988**; c) D. E. Wigley, *Prog. Inorg. Chem.* **1994**, 42, 239.
- [16] a) R. D. Holmes-Smith, S. R. Stobart, R. Vefghi, M. J. Zaworotko, K. Jochem, T. S. Cameron, *J. Chem. Soc. Dalton Trans.* **1987**, 969; b) M. M. Crozat, S. F. Watkins, *J. Chem. Soc. Dalton Trans.* **1972**, 2512; c) V. K. Dioumaev, L. J. Procopio, P. J. Carroll, D. H. Berry, *J. Am. Chem. Soc.* **2003**, 125, 8043; d) E. Sola, A. García-Camprubí, J. L. Andrés, M. Martín, P. Plou, *J. Am. Chem. Soc.* **2010**, 132, 9111.
- [17] R. H. Crabtree, *The Organometallic Chemistry of the Transition Metals*, 5th ed., Wiley, New York, **2009**.
- [18] For selected recent discussions of the *trans* influence in octahedral complexes, see: a) I. Tubert-Brohman, M. Schmid, M. Meuwly, *J. Chem. Theory Comput.* **2009**, 5, 530; b) C. Azerraf, D. Gelman, *Chem. Eur. J.* **2008**, 14, 10364; c) A. E. Anastasi, P. Comba, J. McGrady, A. Lienke, H. Rohwer, *Inorg. Chem.* **2007**, 46, 6420; d) H. Sun, X. Li, H.-F. Klein, U. Flörke, H.-J. Haupt, *Organometallics* **2005**, 24, 2612; e) M. S. Shongwe, C. H. Kaschula, M. S. Adsetts, E. W. Ainscough, A. Brodie, M. J. Morris, *Inorg. Chem.* **2005**, 44, 3070; f) W. Galezowski, M. Kubicki, *Inorg. Chem.* **2005**, 44, 9902; g) F. Baril-Robert, A. L. Beauchamp, *Can. J. Chem.* **2003**, 81, 1326; h) T. Harada, S. Wada, H. Yuge, T. K. Miyamoto, *Acta Crystallogr. Sect. C* **2003**, 59, m37; i) X. Coullens, M. Gressier, M. Dartiguenave, S. Fortin, A. L. Beauchamp, *J. Chem. Soc. Dalton Trans.* **2002**, 3032; j) K. M. Anderson, A. Guy Orpen, *Chem. Commun.* **2001**, 2682; k) D. V. Yandulov, D. Huang, J. C. Huffman, K. G. Caulton, *Inorg. Chem.* **2000**, 39, 1919.
- [19] For a preliminary communication, see: A. Y. Khalimon, S. K. Ignatov, R. Simionescu, L. G. Kuzmina, J. A. K. Howard, G. I. Nikonov, *Inorg. Chem.* **2012**, 51, 754.
- [20] a) T. D. Tilley, in *The Chemistry of Organic Silicon Compounds* (Eds.: S. Patai, Z. R. Rappoport), Wiley, New York, **1989**, Chapter 24; b) T. D. Tilley, in *The Chemistry of Organic Silicon Compounds* (Eds.: S. Patai, Z. R. Rappoport), Wiley, New York, **1991**; for some recent examples, see: c) C. Kayser, G. Kickelbick, C. Marschner, *Angew. Chem.* **2002**, 114, 1031; *Angew. Chem. Int. Ed.* **2002**, 41, 989.
- [21] J. Corey, *Chem. Rev.* **2011**, 111, 863.
- [22] a) A. Y. Khalimon, E. Peterson, C. Lorber, L. G. Kuzmina, J. A. K. Howard, A. van der Est, G. I. Nikonov, *Eur. J. Inorg. Chem.* **2013**, 2205; b) an analogous robust borohydride of Mo has recently been reported: A. Y. Khalimon, J. P. Holland, R. M. Kowalczyk, E. J. L. McInnes, J. C. Green, P. Mountford, G. I. Nikonov, *Inorg. Chem.* **2008**, 47, 999.
- [23] For details, see the Supporting Information.
- [24] a) A. P. Duncan, R. G. Bergman, *Chem. Rec.* **2002**, 2, 431; b) R. A. Eikay, M. M. Abu-Omar, *Coord. Chem. Rev.* **2003**, 243, 83; c) N. Hazari, P. Mountford, *Acc. Chem. Res.* **2005**, 38, 839.
- [25] F. Basuli, B. C. Bailey, L. A. Watson, J. Tomaszewski, J. C. Huffman, D. J. Mendiola, *Organometallics* **2005**, 24, 1886.

- [26] For Group 6 borohydride complexes, see: a) S. W. Kirtley, M. A. Andrews, R. Bau, G. W. Grynkewich, T. J. Marks, D. L. Tipton, B. R. Whittlesey, *J. Am. Chem. Soc.* **1977**, *99*, 7154; b) J. L. Atwood, W. E. Hunter, E. Carmona-Guzman, G. Wilkinson, *J. Chem. Soc. Dalton Trans.* **1980**, 467; c) M. Tamm, B. Dressel, T. Luggler, R. Fröhlich, S. Grimme, *Eur. J. Inorg. Chem.* **2003**, 1088; d) M. Tamm, B. Dressel, T. Bannenber, J. Grunenber, E. Z. Herdtweck, *Natuforsch.* **2006**, *61*, 896.
- [27] Alternatively, complexes **2** and **7** can be prepared by reacting the dichlorides [(RN=)MoCl₂(PMe₃)₂] with L-selectride; for details, see ref. [11b].
- [28] a) G. I. Nikonov, *Adv. Organomet. Chem.* **2005**, *53*, 217–309; b) J. Y. Corey, J. Braddock-Wilking, *Chem. Rev.* **1999**, *99*, 175; c) G. Alcaraz, S. Sabo-Etienne, *Coord. Chem. Rev.* **2008**, *252*, 2395.
- [29] For examples of α -gostic silyl complexes, see: a) A. D. Sadow, T. D. Tilley, *J. Am. Chem. Soc.* **2003**, *125*, 9462; b) B. V. Mork, T. D. Tilley, A. J. Schultz, J. A. Cowan, *J. Am. Chem. Soc.* **2004**, *126*, 10428; c) T. Watanabe, H. Hashimoto, H. Tobita, *Angew. Chem.* **2004**, *116*, 220; *Angew. Chem. Int. Ed.* **2004**, *43*, 218; d) V. M. Iluc, G. L. Hillhouse, *J. Am. Chem. Soc.* **2010**, *132*, 11890.
- [30] H. A. Bent, *Chem. Rev.* **1961**, *61*, 275.
- [31] The elongated Mo1–H1 distance (1.9202 Å) may reflect this unfavorable location of the hydride group *trans* to the imido group (from an electronic point of view). However, care should be exercised in the interpretation of the positions of the hydrogen atoms in heavy-element environments.
- [32] a) A. F. Cotton, J. Wilkinson, C. A. Murillo, M. Bochmann, *Advanced Inorganic Chemistry*, 6th ed., Wiley, New York, **1999**; b) R. H. Crabtree, *The Organometallic Chemistry of the Transition Metals*, 5th ed., Wiley, New York, **2009**; c) C. E. Housecroft, A. G. Sharpe, *Inorganic Chemistry*, 6th ed., Pearson, **2008**; d) *Shriver & Atkin's Inorganic Chemistry*, 4th ed., W. H. Freeman, New York, **2006**.
- [33] For selected examples of fluxional octahedral polyhydride complexes, see: a) E. L. Muetterties, *Acc. Chem. Res.* **1970**, *3*, 266; b) C. Soubra, Y. Oishi, T. A. Albright, H. Fujimoto, *Inorg. Chem.* **2001**, *40*, 620; c) D. M. Heinekey, M. van Roon, *J. Am. Chem. Soc.* **1996**, *118*, 12134.
- [34] For selected examples of fluxional octahedral non-hydride complexes, see: a) G. Santiso Quiñones, K. Seppelt, *Chem. Eur. J.* **2006**, *12*, 1790, and references therein; b) A. A. Ismail, F. Sauriol, I. S. Butler, *Inorg. Chem.* **1989**, *28*, 1007, and references therein; c) A. Rodger, B. F. G. Johnson, *Inorg. Chem.* **1988**, *27*, 3062.
- [35] a) T. I. Gountchev, T. D. Tilley, *J. Am. Chem. Soc.* **1997**, *119*, 12831; b) G. I. Nikonov, P. Mountford, S. R. Dubberley, *Inorg. Chem.* **2003**, *42*, 258; c) S. K. Ignatov, N. H. Rees, A. A. Merkoulou, S. R. Dubberley, A. G. Razuvaev, P. Mountford, G. I. Nikonov, *Chem. Eur. J.* **2008**, *14*, 296.
- [36] For the second step: $\Delta H^\ddagger = 13.8 \text{ kcal mol}^{-1}$, $\Delta S^\ddagger = -9.3 \text{ cal K}^{-1} \text{ mol}^{-1}$.
- [37] Significant decomposition of the complex is observed at higher temperatures.
- [38] C. Naumann, B. O. Patrick, J. C. Sherman, *Tetrahedron* **2002**, *58*, 787.
- [39] B. H. Kim, H.-G. Woo, *Adv. Organomet. Chem.* **2004**, *52*, 143.
- [40] For the reduction of carbonyl compounds into alkanes, see: a) C. T. West, S. J. Donnelly, D. A. Kooistra, M. P. Doyle, *J. Org. Chem.* **1973**, *38*, 2675; b) L. R. C. Barclay, H. R. Sonawane, M. C. MacDonal, *Can. J. Chem.* **1972**, *50*, 281; c) J. L. Fry, M. Orfanopoulos, M. G. Adlington, W. R. J. Dittman, S. B. Silverman, *J. Org. Chem.* **1978**, *43*, 374.
- [41] D. V. Gutsulyak, G. I. Nikonov, *Angew. Chem.* **2010**, *122*, 7715; *Angew. Chem. Int. Ed.* **2010**, *49*, 7553.
- [42] T. Fuchigami, I. Igarashi, *Jap. Patent Appl.* JP11228579 (1999).
- [43] For the catalytic hydrosilylation of imines into amines, see: a) T. Murai, T. Sakane, S. Kato, *J. Org. Chem.* **1990**, *55*, 449; b) T. Murai, T. Sakane, S. Kato, *Tetrahedron Lett.* **1985**, *26*, 5145; c) A. M. Caporosso, N. Panziera, P. Petrici, E. Pitzalis, P. Salvadori, G. Vitulli, G. Martra, *J. Mol. Catal. A* **1999**, *150*, 275; d) I. Cabrita, A. C. Fernandes, *Tetrahedron* **2011**, *67*, 8183.
- [44] For examples of transition metal promoted aldol reactions, see: H. Gröger, E. M. Vogl, M. Shibasaki, *Chem. Eur. J.* **1998**, *4*, 1137.
- [45] The data at 50% conversion were used because, at high conversions, the data can be compromised by the formation of the coupling product (**20**).
- [46] For example, see: a) D. M. Hoffman, D. Lappas, D. A. Wierda, *J. Am. Chem. Soc.* **1989**, *111*, 1531; b) G. Parkin, E. Bunel, B. J. Burger, M. S. Trimmer, A. van Asselt, J. E. Bercaw, *J. Mol. Catal. A* **1984**, *41*, 21; c) T. Tatsumi, M. Shibagaki, H. Tominaga, *J. Mol. Catal. A* **1984**, *24*, 19; d) W. A. Nugent, R. M. Zubyk, *Inorg. Chem.* **1986**, *25*, 4604; e) T. Tatsumi, M. Shibagaki, H. Tominaga, *J. Organomet. Chem.* **1981**, *215*, 67; f) for the related activation of amide, see: J. S. Figueroa, N. A. Piro, D. J. Mindiola, M. Fickes, C. C. Cummins, *Organometallics* **2010**, *29*, 5215.
- [47] A. Y. Khalimon, P. Farha, R. Simionescu, L. G. Kuzmina, G. I. Nikonov, *Chem. Commun.* **2012**, 48, 455.
- [48] a) M. F. C. Guedes da Silva, J. J. R. Frausto da Silva, A. J. L. Pombeiro, *Inorg. Chem.* **2002**, *41*, 219; b) J. E. Bercaw, D. L. Davies, P. T. Wolczanski, *Organometallics* **1986**, *5*, 443; c) G. Erker, W. Frömberg, J. L. Atwood, W. E. Hunter, *Angew. Chem.* **1984**, *96*, 72; *Angew. Chem. Int. Ed. Engl.* **1984**, *23*, 68.
- [49] a) S. S. Yun, T. S. Kim, C. H. Kim, *Bull. Korean Chem. Soc.* **1994**, *15*, 522; b) S. S. Yun, J. Lee, S. Lee, *Bull. Korean Chem. Soc.* **2001**, *22*, 623; c) S. Leelasubcharoen, P. A. Zhizhko, L. G. Kuzmina, A. V. Churakov, J. A. K. Howard, G. I. Nikonov, *Organometallics* **2009**, *28*, 4500.
- [50] For an example of a bis(aldehyde)molybdenum complex, see: C.-S. Chen, C.-S. Lin, W.-Y. Yeh, *J. Organomet. Chem.* **2011**, *696*, 1474.
- [51] For examples of η^2 -coordinated aldehyde complexes, see: I. J. Blackmore, C. J. S. Emiao, M. S. A. Buschhaus, B. O. Patric, P. Legzdins, *Organometallics* **2007**, *26*, 4881.
- [52] P. W. Dyer, V. C. Gibson, J. A. K. Howard, C. Wilson, *J. Organomet. Chem.* **1993**, *462*, C15.
- [53] The Mo–alkyl bond length falls within the range 1.879–2.483 Å (average: 2.208 Å).
- [54] V. Yu. Kukushkin, A. J. L. Pombeiro, *Chem. Rev.* **2002**, *102*, 1771, and references cited therein.
- [55] For examples of η^2 -imino molybdenum complexes, see: a) J. Okuda, G. E. Herberich, *Organometallics* **1987**, *6*, 2331; b) J. Okuda, G. E. Herberich, *J. Organomet. Chem.* **1988**, *353*, 65; c) T. Komuro, R. Begum, R. Ono, H. Tobita, *Dalton Trans.* **2011**, *40*, 2348.
- [56] S. K. Ignatov, A. Y. Khalimon, N. H. Rees, A. G. Razuvaev, P. Mountford, G. I. Nikonov, *Inorg. Chem.* **2009**, *48*, 9605.
- [57] J. P. Banovetz, H. Suzuki, R. M. Waymouth, *Organometallics* **1993**, *12*, 4700.
- [58] SHELXTL-Plus, Release 5.10, Bruker AXS Inc., Madison, Wisconsin, USA, **1997**.
- [59] Gaussian 03 (Revision D.01), M. J. Frisch, G. W. Trucks, H. B. Schlegel, G. E. Scuseria, M. A. Robb, J. R. Cheeseman, V. G. Zakrzewski, V. G.; J. A. Montgomery, Jr., R. E. Stratmann, J. C. Burant, S. Dapprich, J. M. Millam, A. D. Daniels, K. N. Kudin, M. C. Strain, O. Farkas, J. Tomasi, V. Barone, M. Cossi, R. Cammi, B. Mennucci, C. Pomelli, C. Adamo, S. Clifford, J. Ochterski, G. A. Petersson, P. Y. Ayala, Q. Cui, K. Morokuma, D. K. Malick, A. D. Rabuck, K. Raghavachari, J. B. Foresman, J. Cioslowski, J. V. Ortiz, B. B. Stefanov, G. Liu, A. Liashenko, P. Piskorz, I. Komaromi, R. Gomperts, R. L. Martin, D. J. Fox, T. Keith, M. A. Al-Laham, C. Y. Peng, A. Nanayakkara, C. Gonzalez, M. Challacombe, P. M. W. Gill, B. Johnson, W. Chen, M. W. Wong, J. L. Andres, C. Gonzalez, M. Head-Gordon, E. S. Replogle, J. A. Pople, Gaussian, Inc., Wallingford, CT, **2004**.
- [60] a) A. D. Becke, *J. Chem. Phys.* **1993**, *98*, 5648; b) J. P. Perdew, K. Burke, Y. Wang, *Phys. Rev. B* **1996**, *54*, 16533.
- [61] P. J. Hay, W. R. Wadt, *J. Chem. Phys.* **1985**, *82*, 299.

Received: January 30, 2013
Published online: ■ ■ ■, 0000
